SEDIMENTOLOGY the journal of the International Association of Sedimentologists

Sedimentology (2009) **56,** 1905–1936 doi: 10.1111/j.1365-3091.2009.01062.x

High-frequency cyclicity (Milankovitch and millennial-scale) in slope-apron carbonates: Zechstein (Upper Permian), North-east England

MIKE MAWSON and MAURICE TUCKER
Department of Earth Sciences, Durham University, Durham DH1 3LE, UK (E-mail: m.e.tucker@durham.ac.uk)

Associate Editor: Christian Betzler

ABSTRACT

The Upper Permian (Zechstein) slope carbonates in the Roker Formation (Zechstein 2nd-cycle Carbonate) in North-east England consist of turbidites interbedded with laminated lime-mudstone. Studies of turbidite bed thickness and relative proportion of turbidites (percentage turbidites in 20 cm of section) reveal well-developed cyclicities consisting of thinning-upward and thickening-upward packages of turbidite beds. These packages are on four scales, from less than a metre, up to 50 m in thickness. Assuming that the laminae of the hemipelagic background sediment are annual allows the durations of the cycles to be estimated. In addition, counting the number and thickness of turbidite beds in 20 cm of laminated lime-mudstone, which is approximately equivalent to 1000 years (each lamina is 200 μm), gives the frequencies of the turbidite beds, the average thicknesses and the overall sedimentation rates through the succession for 1000 year time-slots. Figures obtained are comparable with modern rates of deposition on carbonate slopes. The cyclicity present in the Roker Formation can be shown to include: Milankovitch-band *ca* 100 kyr short-eccentricity, *ca* 20 kyr precession and *ca* 10 kyr semi-precession cycles and sub-Milankovitch millennial-scale cycles (0·7 to 4·3 kyr). Eccentricity and precession-scale cycles are related to 'highstand-shedding' and relative sea-level change caused by Milankovitch-band orbital forcing controlling carbonate productivity. The millennial-scale cycles, which are quasi-periodic, probably are produced by environmental changes controlled by solar forcing, i.e. variations in solar irradiance, or volcanic activity. Most probable here are fluctuations in carbonate productivity related to aridity–humidity and/or temperature changes. Precession and millennial-scale cycles are defined most strongly in early transgressive and highstand parts of the larger-scale short-eccentricity cycles. The duration of the Roker Formation as a whole can be estimated from the thickness of the laminated lithotype as *ca* 0·3 Myr.

Keywords Carbonate turbidite, Milankovitch cycles, millennial-scale cycles, North-east England, orbital forcing, Permian, slope-apron carbonates, Zechstein.

INTRODUCTION

This paper documents the cyclicity of carbonate turbidites in a slope-apron succession from the Upper Permian of North-east England and interprets this in terms of changes in carbonate productivity and supply caused by relative sea-level and climatic oscillations induced by orbital and solar forcing. The sub-Milankovitch, millennial-scale periodicity that the turbidites

exhibit is of particular interest and significance; cyclicity of this type has rarely been described in the pre-Pleistocene geological record, as the high-resolution stratigraphical control necessary for this generally is lacking. In contrast, millennial-scale, as well as higher-frequency (decadal to centennial-scale), cyclicity is observed in many Quaternary sedimentary records (Fairbanks, 1989; Behl & Kennet, 1996; Hughen *et al.*, 1996a,b; Kennet *et al.*, 2000; Roth & Reijmer, 2005), as well as in polar-ice and tree-ring data. In sedimentary rocks from older geological epochs, millennial-scale periodicity has been documented in only a few instances (Anderson, 1982; Elrick & Hinnov, 1996, 2007; Zühlke, 2004) or is evident but not discussed (Bádenas *et al.*, 2005), whereas the much longer orbital-forcing, Milankovitch-band cycles are recognized widely (e.g. Lehrmann & Goldhammer, 1999).

This paper examines a slope-apron carbonate succession containing turbidites in the Roker Formation of the Zechstein Group from North-east England (Fig. 1). The data collected consist of two basic parameters: (i) the thickness of each turbidite bed; and (ii) the thickness of each unit of 'background' laminated lithotype with which the turbidites are interbedded. The relative thickness of the turbidites is, broadly speaking, inversely proportional to that of the thickness of adjacent laminated units. In other words, sections containing thick turbidite beds are associated with relatively thin units of laminated lithology and vice-versa. This relationship can also be considered in terms of the relative proportions (percentages) of each lithotype in a unit of section. Furthermore, the stratigraphy is organized into packages consisting of upward-decreasing and upward-increasing turbidite bed thickness and percentage. It is this cyclicity that is discussed in this paper. There is no independent information from radiometric age dating, biostratigraphy or magnetostratigraphy on the duration of the Roker Formation. However, the high-resolution time-scale required to establish the duration of the cyclicity present, and in particular to recognize the millennial-scale periodicity, is provided by the laminated lithotype interbedded with the turbidites, where each lamina is interpreted as annual.

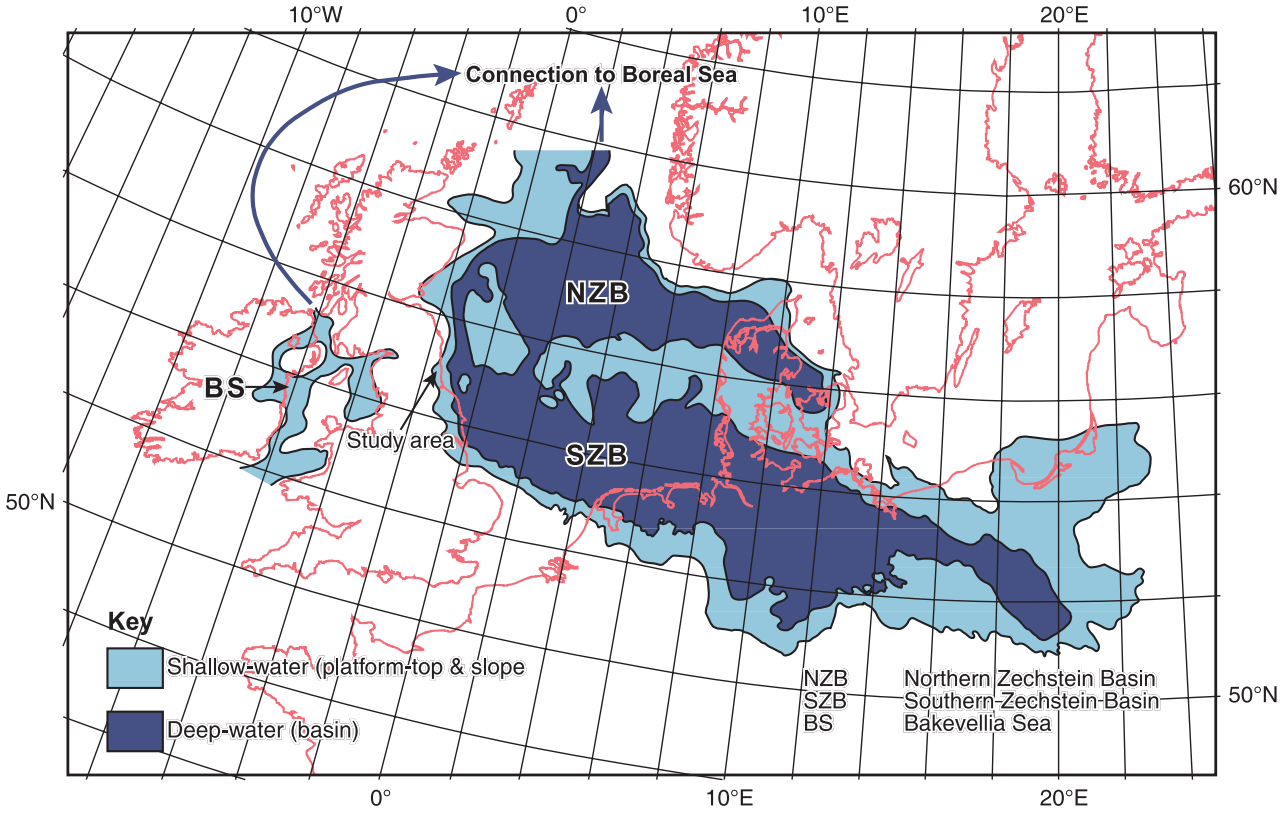

Fig. 1. Palaeogeography in Late Permian time showing the Northern and Southern Zechstein Basins, separated by the mid-North Sea high. Areas of shallow and deep water sedimentation are also shown, as well as the location of the study area.

GEOLOGICAL BACKGROUND

Upper Permian (Zechstein) stratigraphy

The Zechstein Group consists of a thick succession (up to *ca* 2 km) of Upper Permian cyclic carbonates and evaporites, with relatively minor clastics. This succession was deposited within the continental interior of Pangea in a vast intracratonic basin which occupied much of the present-day North Sea and also covered parts of Eastern England and most of northern continental Europe (Fig. 1; Taylor, 1998; Smith & Taylor, 1992). This basin can be divided into two major sub-basins, the Northern and Southern Zechstein Basins (NZB and SZB), in which further, smaller, sub-basins were present (Fig. 1). The study area in the County of Tyne & Wear in North-east England (Fig. 2), was located on the western margin of the SZB (Fig. 1) and is situated in Marsden Bay, near Sunderland (Figs 2 and 3). The formation of evaporite deposits within the basin was promoted by its landlocked nature and subtropical palaeolatitude (*ca* 20°N), as well as the hot, arid climate of the time. The entrance to the Zechstein Sea was also probably silled where it was connected to the open ocean, most probably just with the Boreal Sea to the north. A communication with Tethys to the south-east may also have been established (Ziegler, 1990b; Ziegler *et al.*, 1997). The succession shows a broad upward change from predominantly carbonate to evaporite rocks and the evaporites from sulphate to halite to potash composition. The Zechstein Group represents an early transgressive but largely regressive, succession of around 5 to

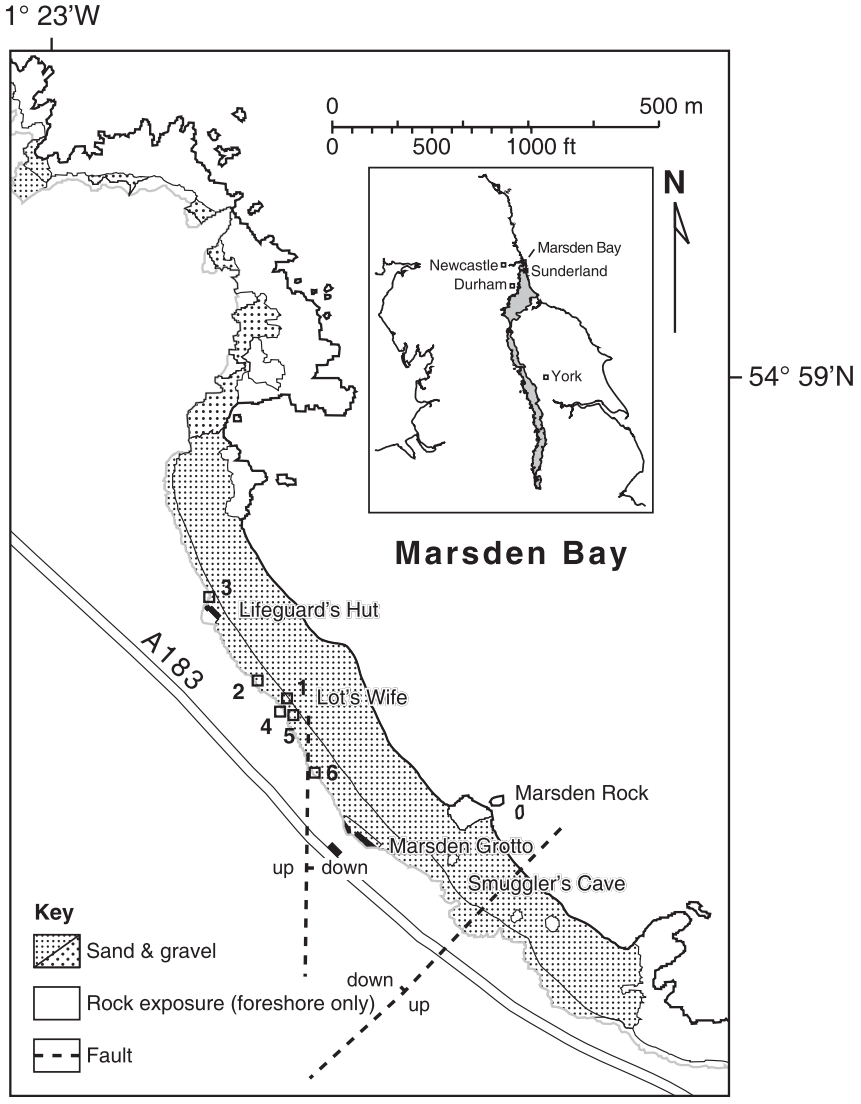

Fig. 2. Location of the study area in North-east England, with outcrop of Upper Permian carbonates, and a map of Marsden Bay showing the position of logs used to construct composite log (data in this study from localities 1 to 6). Two major faults are present; the one to the south of Marsden Grotto may have been active during deposition of the Roker Formation as indicated by facies and thickness changes across it.

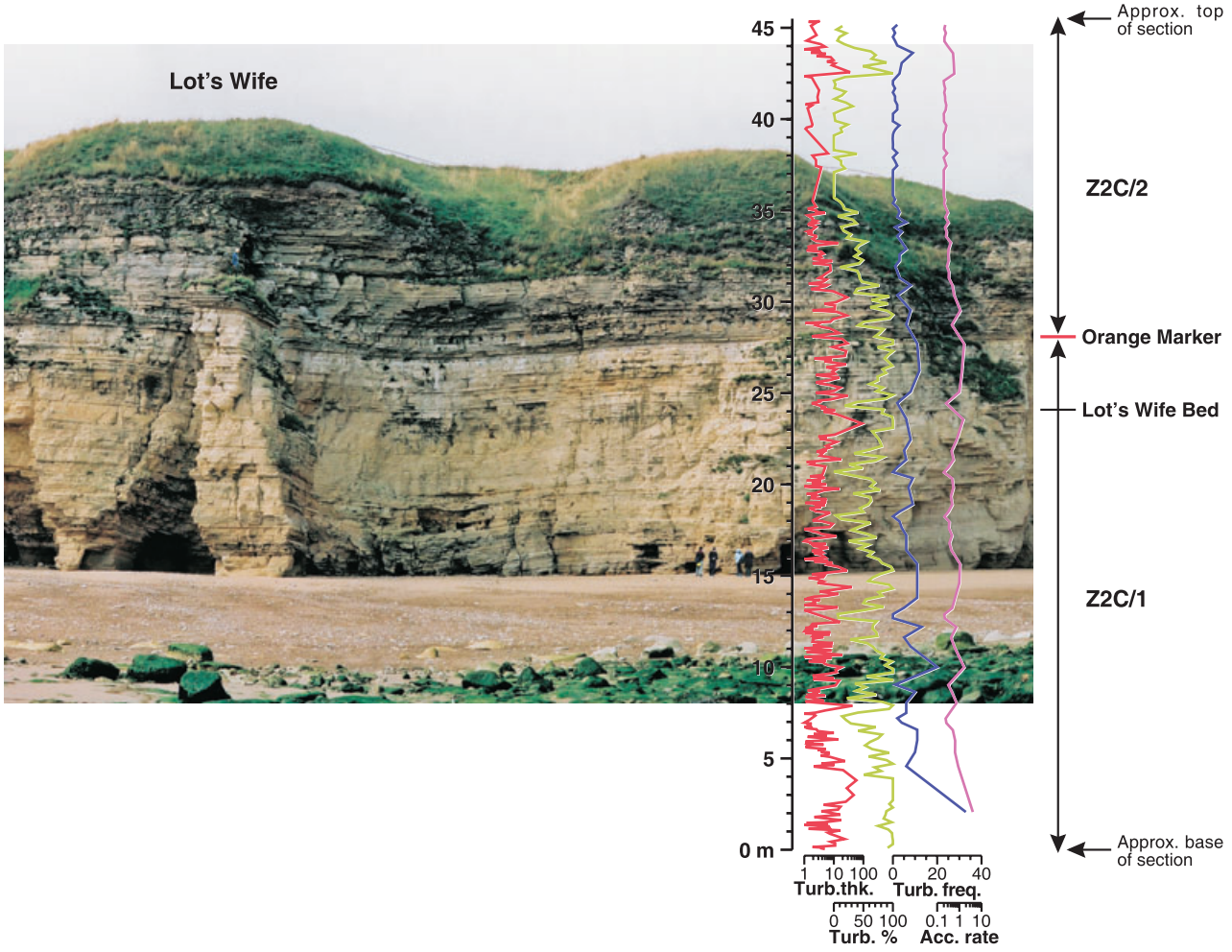

Fig. 3. Exposure of Roker Formation slope-apron rocks in Marsden Bay in the vicinity of Lot's Wife (a sea-stack). Also shown, for the whole section studied, are the plots for turbidite thickness (cm), percentage and frequency (no. kyr^{-1} or 20 cm), as well as the accumulation rate (m kyr^{-1}). See text for explanation. The section for the plots below beach level is *ca* 200 m to the right of cliff (north), and the section for the plots above the cliff is *ca* 100 m to the left (south).

7 Myr duration (Gradstein *et al.*, 2004; Menning *et al.*, 2005).

Traditionally, the Zechstein Group has been divided into carbonate to evaporite cycles (Richter-Bernburg, 1955; Fig. 4), five of which are widely distinguished, as in the study area (Smith, 1989). The carbonates described in this paper belong to the second cycle, i.e. Z2C (Zechstein 2nd-cycle Carbonate) and are termed here the 'Roker Formation'. The validity of the cycle approach is brought into question when the Group is examined from a sequence stratigraphic point of view (Tucker, 1991); the succession is then viewed as a series of sequences generally consisting of lowstand evaporite, transgressive evaporate to carbonate and highstand carbonate, systems tracts (Tucker, 1991). For further information regarding the Zechstein Group see Taylor & Colter (1975), Tucker (1991) and Taylor (1998).

Roker Formation

The 'Roker Formation' is a new term, not yet formally defined which, for various reasons noted in the *Appendix*, is used in preference to the two older stratigraphic divisions for the Z2C in NE England; namely the Concretionary Limestone and the Roker Dolomite. In continental Europe, where it forms a hydrocarbon exploration target, as well as in the UK sector of the southern North Sea, the equivalent of the Roker Formation is the 'Haupt Dolomite' (Rhys, 1974; Taylor, 1998). The Roker Formation is generally up to *ca* 100 m thick

		UK southern N. Sea	UK onshore	
	Triassic	Bunter Shale Fm.	Sherwood Sst. Group	
			Roxby Formation	
Zechstein Group	Z5	Grenz Anhydrite	Littlebeck Anhydrite	Z5A
	Z4	Aller Halite	Sneaton Halite	Z4S
		Pegmatitic Anhydrite	Sherburn Anhydrite	Z4A
		Roter Salzton	Rotten Marl	RS
	Z3	Leine Halite	Boulby Halite	Z3S
		Haupt Anhydrite	Billingham Anhydrite	Z3A
		Platten Dolomite	Seaham Formation	Z3C
		Grauer Salzton		GS
	Z2	Deck Anhydrite	Fordon Formation	Z2Aii
		Stassfurt Halite		Z2S
		Basal Anhydrite		Z2Ai
		Haupt Dolomite	Roker Formation	Z2C
	Z1	Werra Anhydrite	Hartlepool Anhydrite	Z1A
		Zechsteinkalk	Cadeby Formation	Z1C
		Kupferschiefer	Marl Slate	KS
	Rotliegend Group		Yellow Sands	

Fig. 4. Zechstein stratigraphy in the UK southern North Sea (after Rhys, 1974) and UK onshore with proposed short-hand nomenclature on the right. It should be noted that the Z1C at outcrop in North-east England is divided generally into the Raisby and Ford Formations but in fact it would be more correct, in terms of stratigraphic procedure, to regard them as members of the Cadeby Formation.

(attained in the more basinward part of the platform) but it is around half this thickness, *ca* 50 to 60 m, on the platform-top. It overlies the cycle 1 Hartlepool Anhydrite (equivalent to the Werra Anhydrite of Germany), which provided a foundation on which the platform developed and also strongly influenced facies distribution and platform geometry. The Roker platform generally had a distally steepened ramp-like morphology. There is evidence for only minor syn-depositional faulting. The Roker platform-margin was oriented *ca* NW to SE and faced north-eastwards, normal to the direction of prevailing north-easterly (trade) winds (Glennie, 1972, 1982, 1998); i.e. it was located in a windward setting. The abundance of sedimentary structures in the Roker Formation platform-top facies formed by waves and storms indicates that these were important processes influencing sediment distribution and dispersal and, therefore, facies type. Strong seasonality is predicted by Permian global climate models (Crowley, 1994; Kutzbach, 1994; Barron & Fawcett, 1995; Gibbs *et al.*, 2002).

The low diversity of the biota (gastropods, ostracods and three species of bivalves; Smith & Francis, 1967) indicates that sea water in the Zechstein Basin had an elevated salinity and temperature during Z2C times (Taylor, 1998). In the basin centre, the water column probably was stratified and partly anoxic; the interface between the anoxic and oxygenated sea water probably was located around the top of the slope-apron.

The Roker Formation displays an overall shallowing-upward trend and constitutes part of a single third-order sequence. Three smaller-scale packages, equivalent to parasequences and interpreted here as 'fourth-order short-eccentricity cycles', can be identified: Z2C/1, Z2C/2 and Z2C/3 (Fig. 5). A similar number of packages is recognized in Germany (Strohmenger *et al.*, 1996a; Leyrer *et al.*, 1999) and Poland (Peryt, 1986).

The facies and grain types, as well as the diagenesis, in the Roker Formation are remarkably similar to those found in the Z2C elsewhere in the Zechstein Basin as, for example, in the Netherlands (Clark, 1980, 1986; Van der Baan, 1990), Germany (Huttel, 1989; Steinhoff & Strohmenger, 1996; Strohmenger *et al.*, 1996b) and Poland (Peryt, 1986). Four broad facies associations (RK1, RK2, RK3 and RK4) are recognized in NE England and summarized in Table 1: RK1 – the slope-apron facies association and the subject of this paper; RK2 – the offshore, mid-ramp facies association, commonly skeletal mud-wackestone and ribbon rocks; RK3 – an inner ramp, foreshore–shoreface facies association dominated by oolitic grainstones; and RK4 – an inner platform tract of evaporites, terrigenous clastics and peritidal carbonates (constituting part of the Edlington Formation).

METHODOLOGY

The approach used to study the cyclicity of the slope-apron facies in the Roker Formation was first to measure the thickness of each turbidite bed and of each unit of laminated lithology between the turbidites in the succession. Using these data, the changes in the relative proportion (percentage or 'volume') of each lithotype were established. A high-resolution time-scale is provided by the laminated lithotype, if it is assumed that each lamina is annual. With this time-scale, net accumulation rates in cm kyr^{-1}, turbidite frequency kyr^{-1} and average bed thickness kyr^{-1} can be established and used to resolve and then interpret the cyclicity. The use of bed-thickness data has recently been reviewed by Sylvester (2007). The packaging was examined in five different ways, as follows:

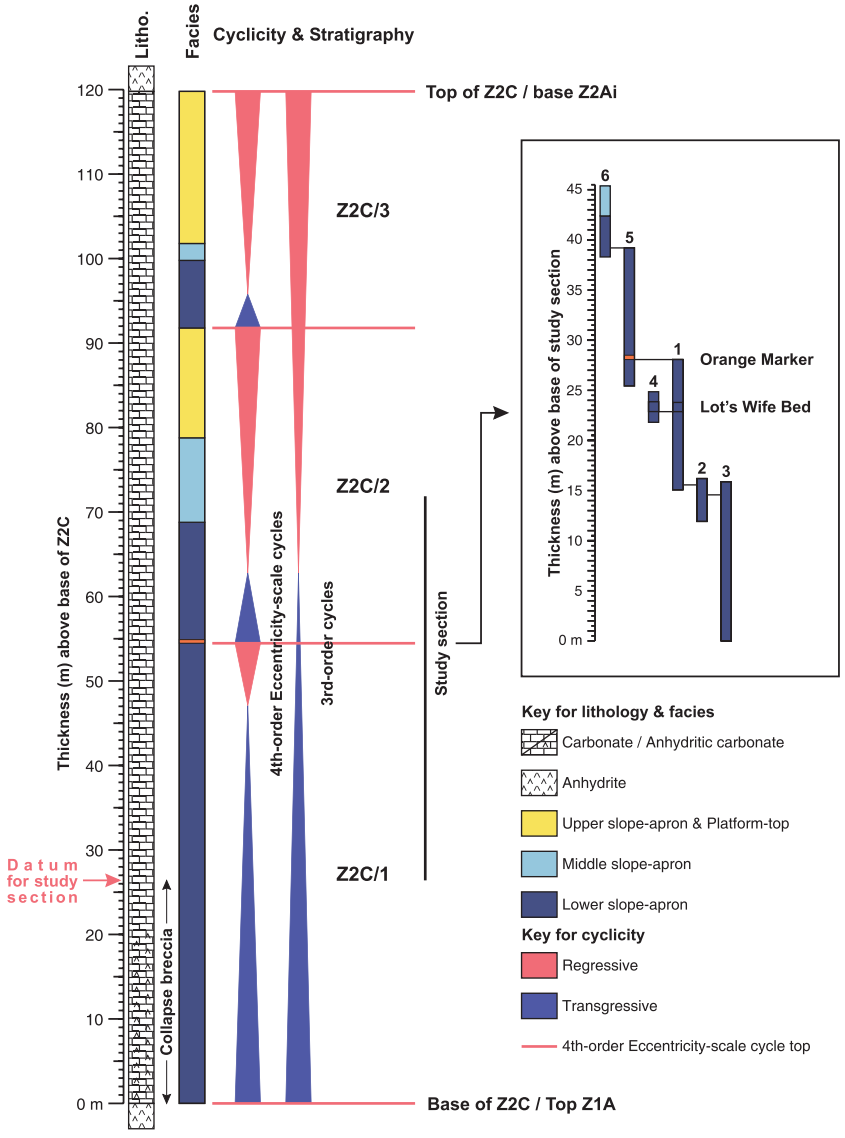

Fig. 5. Schematic diagram of stratigraphy and packages within the Roker Formation at Marsden Bay. Approximately 3 m of collapse breccia probably are present below the base of the study section, reduced from an original thickness of 26 m by the dissolution of anhydrite within it (see text). The packaging above the top of the section discussed, in this paper cannot be determined, as much of it is affected by soft-sediment deformation. The positions of localites 1 to 6 shown in the insert are marked in Fig. 2.

(1) Thicknesses of turbidite beds and laminated units

The thicknesses of individual turbidite beds and units of laminated lithotype in the succession were measured in the field and plotted against stratigraphic thickness.

(2) Percentage of turbidite beds and laminated units

This method examines the relative proportion of the two lithotypes as a percentage. This analysis was undertaken by dividing the stratigraphy into equal units of thickness starting from the base. The sum of each lithotype in each unit was then determined. Units of 5, 10, 20, 25, 30 and 50 cm thickness were considered. This method, which produces a time series, does not recognize bed or unit integrity, so that, for example, a single, thick turbidite bed could occur in more than one thickness division.

(3) Net rate of accumulation

This method is similar to method (2) above but the succession is divided into equal intervals of time, instead of thickness, again starting from the base. In this instance, time is determined from the thickness of the laminated lithotype, on the assumption that laminae were annual. Units containing 5, 10, 20, 25, 30 and 50 cm of the laminated lithotype were examined; these correspond to 0·25, 0·5, 1·0, 1·25, 1·5 and 2·5 kyr, respectively, if mean lamina thickness is 200 μm. The actual thickness of each such division will vary according to the amount of

Table 1. Summary of Roker Formation facies associations and their most characteristic facies. Rocks of RK1, the slope-apron facies association, are the subject of this study.

Facies association	Facies
Platform-top	
RK4: Shallow-water marine to continental*	Interbedded terrigenous claystone and breccia consisting of carbonate clasts. Originally comprised of evaporites (sulphate), mudrock and carbonates; evaporites removed by dissolution and proved in subsurface. Shallow-marine to supratidal sabkha.
RK3: Shallow-water, shoreface and inner ramp	Very coarse to fine-grained ooid grainstone (shallow to very shallow-water, subtidal to intertidal, high to moderate-energy facies). Medium-bedded to thickly-laminated heterolithic sediments with variable proportion of very fine micritic carbonate as thin beds, laminae, lenses and drapes. Stromatolites of varied size and morphology (shallow-water, subtidal, high to moderate energy facies). Planar laminated stromatolitic rocks containing many vugs. Very coarse-grained pisolite (supratidal, moderate energy facies). 'Meteoric' compaction common. Sparse fossil biota. Mostly dolomitized.
Offshore	
RK2: Offshore, middle ramp	Ribbon-rocks: very thin to medium well-bedded lime-mudstone to wackestone containing bivalves, gastropods, ostracods and foraminifera. Thick to very thick units of lime-mudstone to wackestone. Concretionary fabrics (dedolomite) relatively common. Some soft-sediment deformation (probably related to synsedimentary faulting).
RK1: Slope apron	Interbedded units of finely, evenly hemipelagic lime-mudstone and thin to thick unlaminated beds predominantly of lime-mudstone (turbidites). Very thick units of very fine to fine grainstone and packstone and lime-mudstone. Slump-breccias. Soft-sediment deformation very common. Extremely rare well-preserved fossil fish in laminated lithotype. Transported biota in other rock types; most fragmentary and consisting of bivalves and gastropods. Concretionary fabrics (dedolomite) very common.

*Could be assigned to the Edlington or Fordon Formation.

turbidite it contains. This approach provides quantitative data regarding net rates of accumulation, i.e. of turbidite plus laminated lithotype, assuming that small-scale erosion and sediment by-pass were minimal.

(4) and (5) Turbidite frequency and average turbidite bed thickness

The total number of turbidite beds can be counted in each equal interval of time. The divisions used were the same as for method (3); i.e. each unit containing 5, 10, 20, 25, 30 and 50 cm of the laminated lithotype. This method gives a measure of turbidite frequency (4). For each unit, the total number of turbidites and the number of turbidites ≥1 cm were recorded. Note that frequency data quoted are for turbidites ≥1 cm thick unless stated otherwise. Using data from method (3), the average thickness of the turbidites in each time interval was also determined (5).

For method (2), 20 cm of section was used and for methods (3), (4) and (5), the data from 20 cm thick units of the laminated lithology were found best to smooth random signatures in the record. For methods (3), (4) and (5), this unit thickness corresponds to a time interval of *ca* 1 kyr, if mean lamina thickness is 200 μm.

Data regarding compositional changes of the turbidites to complement the thickness analysis would be much harder, if not impossible, to obtain. For example, unlike many Quaternary studies, changes in mineralogy (e.g. aragonite % or calcite %) or isotope values (such as $\delta^{18}O$) could not be examined, because of the diagenetic alteration of the rocks, which is severe locally. All the rocks have been dolomitized and many have subsequently been calcitized (dedolomitized), producing unusual concretionary fabrics in some instances. For the same reasons, differences in the composition of grains and grain-size in the turbidites are hard to establish, although there is some evidence that this signal is present. A technique that could be applied in future is an examination of the palynomaceral content of the turbidites and the laminated lithotype (cf. Strohmenger *et al.*, 1996b). Spectral analysis also would allow further interpretation of the data.

Time-scale

Estimates for the duration of the cyclicity from the thickness of laminated lithotype units interbedded with the turbidites can be used to derive a time-scale, assuming that every lamina is annual. This interpretation has already been proposed by Huttel (1989) and Smith (1994), who suggested that the partings are the product of yearly (summer) blooms of planktonic algae and bacteria. Although convincing evidence is not available to substantiate this suggestion, the strong similarity of these rocks to other laminated lithotypes (Scholle *et al.*, 1983; Anderson, 1996; Hughen *et al.*, 1996a,b), proven to consist of varve couplets, does indicate that an annual origin for them is very likely as well.

In the field, the mean thickness of the laminae in each laminated unit was estimated when logging the section using a standard grain-size card. For hand-samples, the same method was employed or a binocular microscope was used to count the number of laminae in each millimetre or centimetre division of a ruler. Thin-section measurements supplemented these data. Lamina thickness mostly varies from *ca* 150 to 250 μm and an average of *ca* 200 μm is used in this study. With this thickness, 1 cm of laminated lithology corresponds to 50 years and 20 cm to 1000 years (1 kyr). For the most part, lamina thickness is fairly uniform throughout the section studied; the few departures are accounted for in the interpretations. The realistic values obtained in this study for rates of sedimentation and turbidite frequency suggest that the methodology is appropriate.

Problems inherent with the basic data

Firstly, it is hard to establish the correct stratigraphic order and thickness of units in horizons affected by syn-sedimentary creep and slump-folding, as these processes cause repetition and thickening of the stratigraphy. Units affected in this way (particularly thicker ones) probably give an under-estimate of the thickness of laminated lithology, because, when strongly deformed, this lithotype is hard to recognize. Soft-sediment deformation, however, is only significant in middle slope-apron facies (Table 2) where slurrying is also an important process. In contrast, only a relatively small thickness of stratigraphy (*ca* 10%) in the lower slope-apron facies is affected by soft-sediment deformation; these units tend to be thin (<10 cm thick) and/or of limited extent and so do not seriously affect the data. At Marsden Bay, four relatively thick and laterally persistent 'slump-sheets' occur within the lower slope-apron facies of which two are exceptionally thick (2·3 m and 1·2 m). Significant thickening (possibly by over 100%) and repetition of the 'original' stratigraphy by slump-folding have probably occurred in both. Thus the recorded thickness of laminated lithology in each slump-sheet probably is incorrect. The lower of the two slump-sheets also contains a 'slump-breccia' at its base and this is regarded as a turbidite for the purposes of this study.

A second factor which must be considered is that some stratigraphy could be missing or repeated as a result of syn-sedimentary sliding or faulting. This problem is of little importance in the lower slope-apron facies because typically few, minor syn-sedimentary faults are present. In contrast, many syn-sedimentary slides and normal faults (large and medium-scale) occur in the middle slope-apron facies; this partly explains why only 3 m of these strata could be examined for this study.

A third problem inherent in the basic data is that the amount of erosion by turbidity currents is hard to quantify. The fact that many turbidites contain fragments of partings derived from the laminated lithotype indicates that at least some scouring took place and that, as a result, the time-scale provided by the laminated lithology has very probably been shortened. The amount, however, is considered to be relatively insignificant because most of the turbidite beds have flat bases and exhibit only very minor scouring. Units of laminated lithology also display no major thickness changes when traced laterally over nearly 800 m, the limit of the exposure. The amount eroded will probably be greater in units containing a higher volume of turbidites and/or coarser-grained turbidites, i.e. in the middle slope-apron facies.

The stratigraphy of a *ca* 7 m thick unit towards the top of the succession was derived from field photographs, as it could not be measured directly. This derivation has probably introduced a small error into the basic data by under-estimating the thickness of units.

Thus, if, for any of the above reasons, the recorded thickness of the laminated lithotype is less than the original, the time-scale will be shortened; this will have two consequences. Firstly, the cyclicity will appear to be of shorter duration (even that of a higher-frequency cycle) and, secondly, rates of sedimentation will be increased.

Table 2. Slope-apron lithotypes and facies in Facies Association RK1 of the Roker Formation. Details of the three types of laminated lithotype, L1 to L3, are given in Table 3.

Facies	Lithotypes	Soft-sediment deformation	Interpretation/remarks
RK1c	Poorly to very poorly bedded. Crudely interbedded. Thick to very thick massive units of very fine to fine-grained packstone to grainstone (composed of fine ooids) and coarse packstone containing aggregate grains, skeletal material and lithoclasts. A few units of matrix to clast-supported breccia with coarse to very coarse-grained matrix. Units of thickly laminated/very thinly bedded, predominantly fine-grained lime-mudstone; individual layers normally graded.	Pervasive soft-sediment deformation as in Rk1b. Many units affected by creep and slurrying.	Facies RK1c only seen at one locality (Marsden Bay) where it overlies Facies RK1b and underlies platform-top middle ramp rock-types of Facies Association RK2. Lack of finely laminated lithotype and absence of bioturbation indicates dysaerobic environment, unlike that of RK1a and Rk1b; this also indicates depositional setting higher-up slope-apron. A moderate to high-angle of declivity indicated by degree and style of soft-sediment deformation.
RK1b	Poorly to well-bedded. Interbedded units of thinly to thickly laminated lithotype L3 (hemipelagic) and massive, normally graded beds (turbidites), as in RK1a, but coarse-grained or very coarse-grained wackestone to packstone textured beds more common; contains comminuted skeletal material, lithoclasts (of lime-mudstone) and ooids.	Pervasive soft-sediment deformation which affects up to *ca* 50% of stratigraphy. Slurrying very common. Large to medium-scale disconformity surfaces and small to medium-scale syn-sedimentary normal faults. Massive units often boudinaged. Slump-folding.	Middle slope-apron with moderate angle of declivity. High proportion of strata affected by soft-sediment deformation; its extensional style indicates a higher angle of declivity for RK1b than for RK1a; this is also suggested by the more grainy texture of the turbidite beds which also indicates a more proximal setting. Preservation of lamination in laminated lithotype indicates anoxic environment.
RK1a	Well-bedded. Interbedded thinly laminated lithotype L1 (hemipelagic) and massive, normally graded beds (turbidites) 1 to 20 cm thick mostly consisting of lime-mudstone. Some beds of fine to very coarse-grained wackestone to packstone containing poorly preserved ooids and lithic fragments. Fragments of partings from laminated lithotype very common. Partings and thin units of clay-rich, crudely laminated lithotype L2 (pelagic). A few units of 'slump breccia' up to *ca* 80 cm thick in units affected by soft-sediment deformation.	Affects around 10% of stratigraphy. Creep and slump-folding very common in units generally less than 30 cm thick; thickest recorded *ca* 1·8 m thick; this and a few other units associated with 'slump breccias'. A few small-scale syn-sedimentary normal faults.	Lower slope-apron with relatively low angle of declivity; this is indicated by small thickness of stratigraphy affected by slumping and lime-mud-rich nature of sediments. Compressive style of soft-sediment deformation also indicates location near base of slope-apron. Muddy character of most of the turbidite beds, as well as position at base of succession, indicates distal setting relative to other RK1 facies. Anoxic environment suggested by preservation of laminae and organic-rich nature of laminated lithotype.

FACIES ANALYSIS OF THE ROKER (Z2C) SLOPE-APRON

Two principal lithotypes, laminated lime-mudstone and turbidites, occur within the slope-apron facies association (RK1; see Figs 6 and 7). Three separate facies can be differentiated, representing the lower (RK1a), middle (RK1b) and upper (RK1c) slope-apron environment (Table 2).

Laminated lime-mudstone lithotype (laminites)

Description

There are three sub-types of the laminated lithotype (L1, L2 and L3) which are characterized by thin and very even laminae (Table 3, Fig. 8). The most common of these, L1 (Fig. 8A and B), consists of fine, varve-like couplets comprising lighter, generally thicker laminae (25 to 250 μm thick)

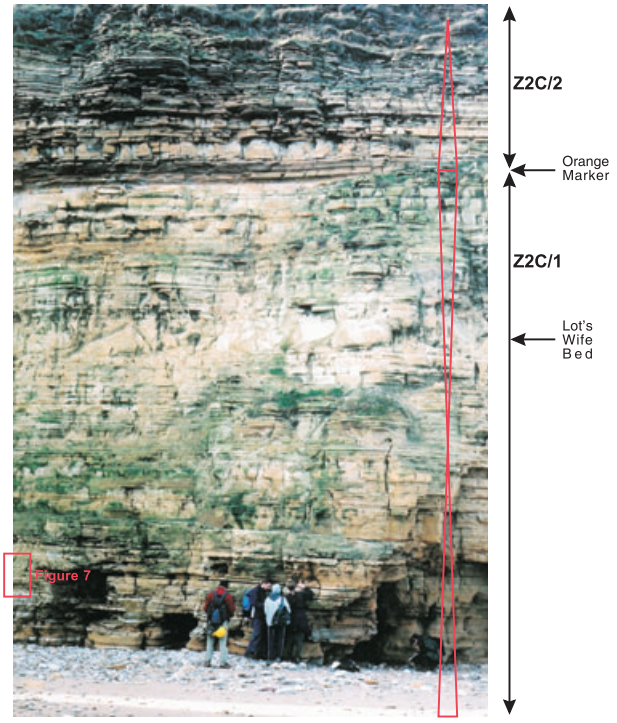

Fig. 6. General view of Roker Formation slope-apron facies, near Lot's Wife Bed, Marsden Bay. Students for scale, maximum height 1·8 m. Turbidite beds are lighter coloured and weather positively relative to the laminated lime-mudstone. The stretched-out vertical triangles on the right show broad trends of turbidite bed thickness and percentage (upward-thinning – decreasing/upward-thickening – increasing). Parts of two large-scale packages (interpreted as the result of short-eccentricity), the upper part of Z2C/1 and lower part of Z2C/2, are exposed here, below and above the Orange Marker, respectively. Below the Orange Marker is the higher frequency cycle (interpreted as the result of precession), Z2C/1i; above the Orange Marker is the lower part of another higher frequency cycle, Z2C/2i. In this view, the base of the cliff is approximately +15·6 m above the base of the studied section. Red box indicates location of Fig. 7.

composed of silt-grade carbonate that alternate with darker partings composed of terrigenous clay admixed with organic material (25 to 70 μm thick). The partings are affected, to varying degrees, by compaction-related dissolution. Palynological studies show that the organic material in the partings contains a low diversity of palynomacerals that are largely of marine origin, although there is also some terrestrially derived material (Fensome, 2002). Total organic carbon (TOC) values (bulk analyses of outcrop and subsurface material) are all below 1% (Fensome, 2002).

Petrographic study shows that the L1 laminae contain small, approximately spherical, peloids 25 to 70 μm in size; these may have been flocs of carbonate mud. A few detrital quartz grains are also found in the partings, always in higher abundance than in adjacent laminae, however. The quartz grains are sub-rounded to sub-angular, mostly silt-sized and are thought to be of aeolian origin. The partings also contain pyrite and trace amounts of mica. Very rare remains of fossil fish, exquisitely preserved, and land plants are also recorded (Kirkby, 1863, 1864; Howse, 1880; Pettigrew, 1980); no benthic biota, either *in situ* or transported, is found. In some thin sections, the laminae display normal grading.

The thickness of each couplet in L1 laminae is generally *ca* 150 to 250 μm. The thickness and sharpness of the laminae and, to a lesser extent, of the partings, do vary. In the field, this variation is expressed by colour differences of layers (lighter and darker shades of brown) within the laminated units. These different coloured layers are up to *ca* 1 cm thick and probably record an even higher-frequency, shorter-duration (decadal-scale) cyclicity.

Another laminated lithotype, L2 (Fig. 8C), occurs in association with L1. The laminae generally are thinner than L1 and more poorly defined. The partings are slightly thicker and contain a high abundance of quartz grains. This rock has a distinctive brown colour and is clay-rich. L1 also is gradational in character with, and generally passes upwards into, a further laminated lithotype, L3 (Fig. 8D). Here, the laminae are thicker, mostly >0·5 to 1·0 mm, and grading is well-defined. This lithotype is only present in the top *ca* 6 m of the section examined; it is typical of the middle slope-apron facies.

Interpretation

In view of their occurrence in the more basinward, mid-slope to outer-slope parts of the Roker Formation, the various laminated lithotypes are considered to have accumulated in substantial water depths, below the influence of fair-weather and storm-generated waves, as 'background' hemipelagic sediment. The preservation of fine lamination, together with the occurrence of organic matter, indicates an anoxic environment, as does the pyrite present. The laminae (couplets) are interpreted as annual in origin.

Turbidite beds

Description

Unlaminated beds, thought to be the product of turbidity currents, are found nearly always

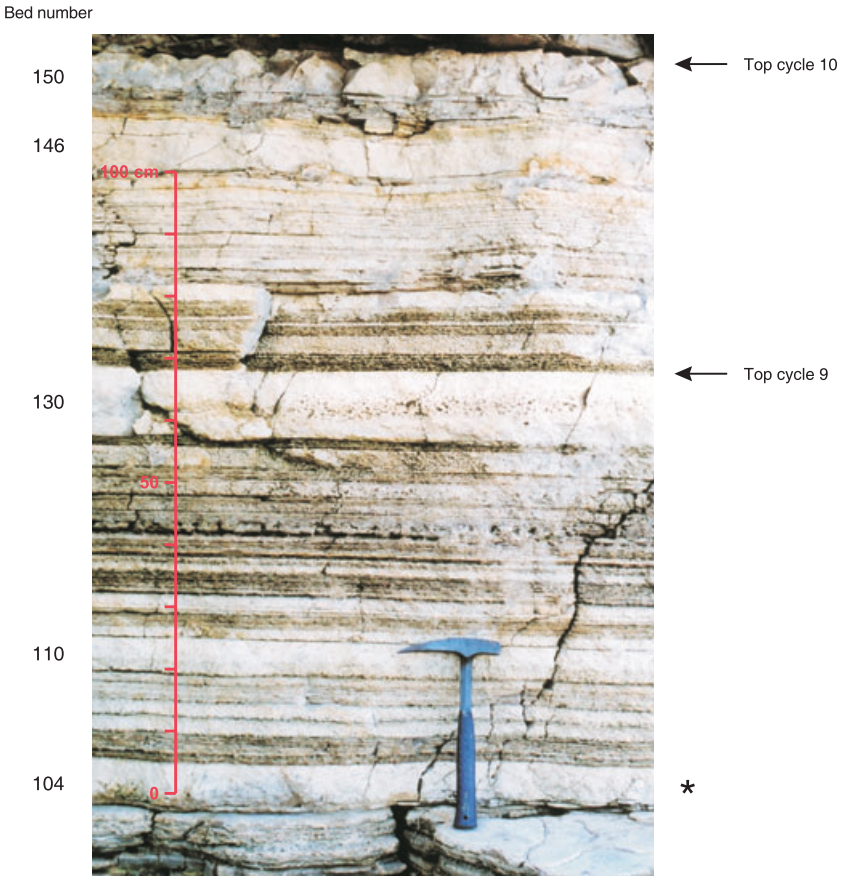

Fig. 7. More detailed view of Roker Formation lower slope-apron (RK1a) facies consisting of interbedded, darker, laminated lime-mudstone and lighter turbidite beds. The section in this view (location shown in Fig. 6) is composed of limestone (dedolomite) with concretionary fabrics from dedolomitization. Patterns of upward-increasing/upward-decreasing turbidite bed thickness and percentage at various scales are readily apparent here. The smallest-scale packages, two of which are seen in this photograph (cycles 9 and 10 of Fig. 12, Table 4), are interpreted as millennial-scale in duration (1 cm of laminated lime-mudstone is approximately equivalent to 50 years). Bed no. 104 (marked with an asterisk) may mark the boundary between two even higher frequency packages within Cycle 9. Cliff near Lot's Wife, Marsden Bay (section shown is from +16·6 to 17·9 m above base of section). Bed numbers are the same as those as indicated on Fig. 13. Hammer is 33 cm long.

Table 3. Finely and evenly laminated lithotypes (L1 to L3) in Roker Formation slope-apron facies.

Type	Description	Facies
L3	Thinly to thickly laminated; sharp to diffuse. Couplets generally 0.5 to 1.0 mm thick; laminae up to 5 mm. Laminae predominantly thicker than in L1 and grade from silt-size to micritic carbonate. Rock often fissile, breaking along partings.	RK1b (middle slope-apron)
L2	Generally very thinly to indistinctly laminated. Terrigenous clay-rich, with distinctive brown colour. Laminae very thin or poorly defined, often discontinuous so that partings often appear thicker than in L1 or L3. Contains a much higher abundance of detrital quartz grains than L1 or L3. Many associated thicker laminae and massive beds contain admixed clay. Only exposed in the vicinity of Marsden Bay, near base of Roker Formation.	RK1a (lower slope-apron)
L1	Thinly to very thinly laminated; sharp to diffuse. Couplets generally 150 to 250 μm thick. Grading of laminae visible in some thin-sections and defined by decrease in proportion of peloids; top of laminae composed of dark micritic carbonate. Some units of laminated lithotype have pale pink-orange colour due to admixed clay.	RK1a (lower slope-apron)

interbedded with the laminated lithotypes described above (as in Figs 6 and 7). Although many such units are less than 1 cm thick and therefore should be referred to as 'laminae' (Tucker, 2003a), for clarity all these units are termed 'beds'. These beds are relatively thin, predominantly 1 to 10 cm thick. The average thickness at Marsden Bay is 3·9 cm for all beds (n = 642) and 5·8 cm for those ≥1 cm thick (n = 414). Of the beds ≥1 cm thick, only 55 (13·3%) are >10 cm thick; 18 (4·5%) are >20 cm thick and just six (*ca* 1·5%) are >30 cm thick (Fig. 9). The thickest bed recorded in the study area is *ca* 1 m thick and, being very distinctive on this account, is named the 'Lot's Wife Bed' (seen in Figs 3 and 6).

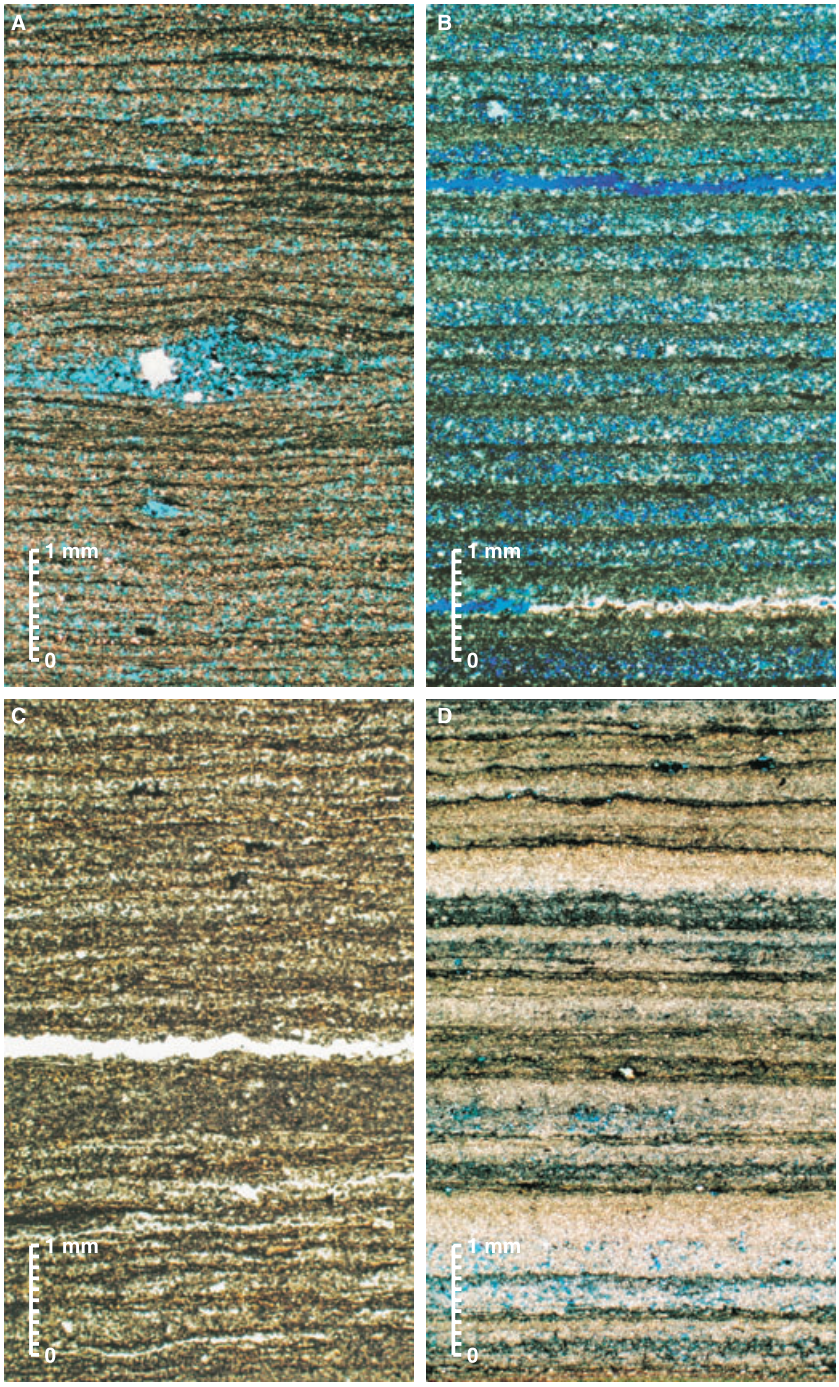

Fig. 8. Laminated lime-mudstones in the slope-apron facies association (RK1) at Marsden Bay. Figures in brackets give location of sample above base of section. (A) Lithotype L1 (+15·9 m); note vug after burial anhydrite. (B) Lithotype L1 (+21·7 m); note normal grading within laminae. (C) Lithotype L2 (+19·9 m). (D) Lithotype L3 (from stratigraphic level above top of studied section). Blue is porosity.

The laminae and turbidite beds do not form a continuum; they belong to two discrete thickness populations with their boundary lying somewhere between 250 and 500 μm. For practical purposes, however, laminae ≤1 mm thick are regarded as being of the laminated lithotype and laminae >1 mm are interpreted as turbidites.

Most of the turbidite beds (even the thickest) are fine-grained, lime-mudstone textured and composed largely of silt-grade carbonate mud (Fig. 10). In most instances, the mud contains small peloids and quartz grains identical to those in the laminated lithotype. The quartz, although ubiquitous, always occurs in much lower abundances (trace amounts; *ca* 1% to 2% of bulk volume) than in the laminated lithotype. Some beds also contain a significant amount of terrigenous clay, giving the bed an orange or chocolate-brown colour, either admixed with the lime-mud or as a discrete, finer fraction towards the top of

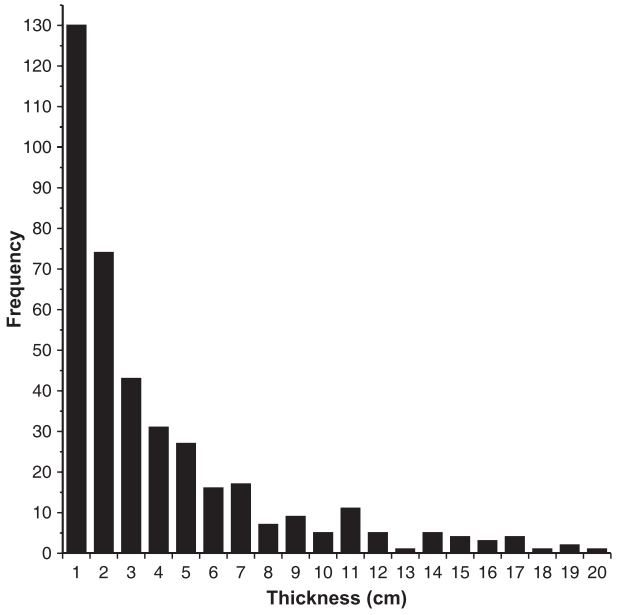

Fig. 9. Histogram of thickness distribution of beds ≥1·0 cm thick (n = 414). Not shown are 18 beds >20 cm thick. 228 beds are <1·0 cm thick.

individual beds. In addition to mudstone, wackestone–packstone textures also occur. In the majority of beds, even the thickest, lime-mudstone-textured rock predominates. For example, in the *ca* 1 m thick Lot's Wife Bed, the packstone layer at its base is only 6 cm thick and this grades upwards rapidly into lime-mudstone which constitutes the rest of the unit.

Excepting the grains seen only in thin section (the fine peloids and quartz grains), grains are largely of four types, in order of abundance:

1 Flake-like grains which clearly are fragments of partings derived from the laminated lithotype (Fig. 10A and B).

2 Non-skeletal grains preserved as equant, vuggy pores, which probably are enlarged moulds, most of which are considered to be ooids on the basis of their size and shape (Fig. 10A). As these grains are very poorly preserved, it is hard to establish their type (i.e. thickness and fabric of their coating) but most appear to be relatively small (<0·2 mm) and quite unlike the ooids that are typical of the shallow-water, high-energy facies (RK3, Table 1) in the Roker Formation.

3 Lithic fragments predominantly with a massive, lime-mudstone texture. From their shape, some are probably of the laminated lithotype; most are relatively small (up to 2 mm) but they can be up to centimetre size.

4 Skeletal material, mostly consisting of broken bivalve fragments, although the origin is often hard to establish because it is so comminuted.

Many of the beds display the same broad set of divisions but they may not always be present. A complete succession, from the base, consists of the following parts: (i) a very gently scoured base (generally <1 mm relief); (ii) packstone to wackestone containing vuggy pores thought to be ooids; (iii) packstone to wackestone containing many

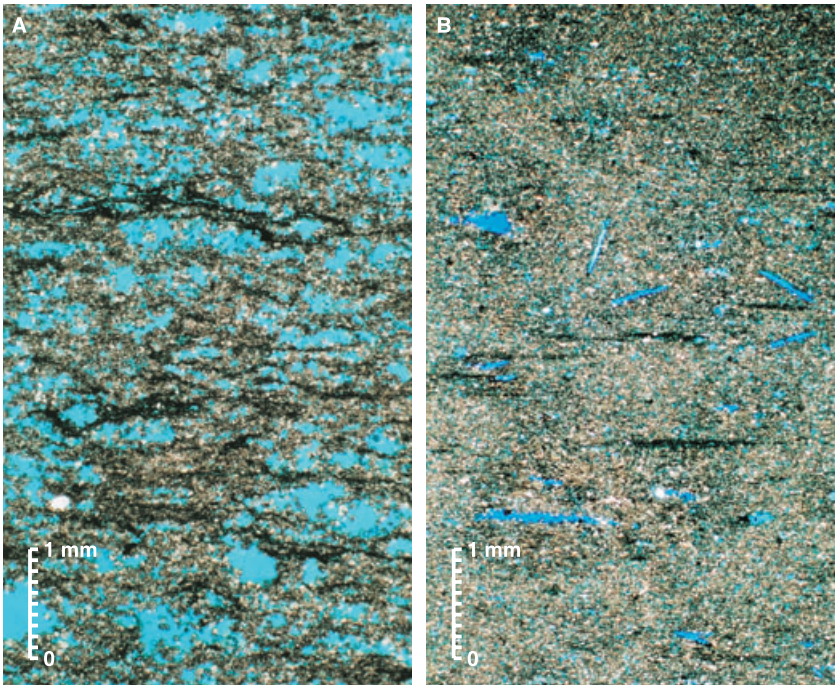

Fig. 10. Photomicrographs of textures present in turbidite beds of lower slope-apron facies (RK1a) at Marsden Bay. Figures in brackets give location of sample above base of section (m). (A) Packstone, division 2 (+13·9 m); vugs are thought to be ooid moulds enlarged by weathering; compacted flakes visible. (B) Flake mudstone – wackestone, division 3 (+22·1 m), with moulds of anhydrite needles. Blue is porosity.

flakes derived from partings; (iv) structureless lime-mudstone to wackestone with few flakes; (v) a finer (silt to clay grade) top, generally very thin, which can consist of porcellaneous (cryptocrystalline) micritic dolomite, terrigenous clay or admixtures of both; and (vi) a sharp, planar top. Parts (iii), (iv) and (v) show a strongly gradational relationship. In many of the turbidite beds, part (ii) is absent and part (v) is hard to discern; most beds consist just of parts (iii) and (iv). There is a broad, positive correlation between the thickness of each unit and texture/grain-size, as well as the degree of scouring. Most beds are single, although a few are composite or amalgamated. The beds also display good lateral continuity. The maximum distance proved is *ca* 0·8 km (limited by exposure) over which there are no significant lateral changes of thickness, texture or grain-size.

Interpretation

These beds are interpreted as the product of turbidity currents as they clearly consist of transported sediment (as indicated by grading, evidence of scouring at their base and the presence of shallow-water grains, such as ooids) and they are interbedded with the laminated lithotype. The sharp, planar contacts of these beds preclude them from being formed by bioturbation of the laminated lithotype. In addition, they and the laminated lithotype interbedded with them, also lack sedimentary structures associated with storm deposits. However, there is a possibility that some, or possibly even most, of these beds could be the product of hyperpycnal flows. Hyperpycnal flows would very probably have formed at the platform-margin/upper slope-apron and, lasting for days or even longer periods of time, could have been generated by major storms (Wilson & Roberts, 1992, 1995; Roth & Reijmer, 2005; Shanmugam, 2008) or by seasonal variations of storm frequency and intensity and/or wind direction and strength, as well as by an increase of sea water salinity. The lack of sedimentary structures such as climbing ripples and, more significantly, of inverse grading (Mulder *et al.*, 2003), both features typical of hyperpycnal deposits, indicates, however, that these beds are more likely to be 'genuine' turbidites. However, it is possible that the absence of such features is due to the different hydrodynamic properties of carbonate sediments and grains relative to their siliciclastic counterparts and/or the fine-grained and uniform nature of the sediment of which most of the beds are constituted. These characteristics would also explain the difficulty in recognizing Bouma divisions within the beds. The only 'true' turbidite deposits then, might be the relatively few units (generally >20 cm thick) which contain relatively coarser-grained material such as ooids (e.g. the Lot's Wife Bed). Although of sedimentological interest, in the context of this paper, the interpretation of these beds as turbidites or hyperpycnites is not significant, as both result from the basinward transport of platform-top sediment, and the fundamental controls on this will most probably be the same. Hereafter, for brevity, these beds are referred to as 'turbidites'.

The slope-apron facies association

The interbedded laminated lime-mudstones and turbidite beds, constituting facies association RK1 are interpreted as slope-apron deposits on the basis of their basinward distribution, common association with soft-sediment deformation and the fact that they grade upwards into offshore, platform-top, middle-ramp facies of RK2. The slope-apron facies association in the Roker Formation can be sub-divided into lower, middle and upper slope apron facies (RK1a, RK1b and RK1c, respectively) on the basis of proximality trends and/or slope declivity, using four criteria, namely: (i) abundance of shallow-water grains and textures in the turbidites; (ii) thickness of laminae in the laminated lithotype; (iii) other facies types present; and (iv) style and degree of gravity-driven, down-slope soft-sediment deformation. The features of these slope-apron facies are given in Table 2.

The profile of the Z2C slope-apron varied in time and space but most of RK1 appears to have been deposited in a relatively distal location on a uniform, low-angle slope, i.e. in a lower slope-apron setting. This observation is indicated by the mud-rich nature of the turbidites and the fine and even character of the laminae in the laminated lithotype, as well as the relatively small thickness of stratigraphy affected by soft sediment deformation.

Within the Z2C of the Sunderland area, units of slope-apron facies (RK1) (Table 3) occur in each of the three smaller-scale packages (Z2C/1, Z2C/2 and Z2C/3). The relative thickness of each unit of RK1 decreases successively in each of these three packages, from *ca* 28 m in Z2C/1, to *ca* 14 m in Z2C/2 and to *ca* 8 m in Z2C/3. In each package, a general upward increase in grain-size and abundance of shallow-water derived grains is observed, concomitant with an increase in the abundance of grain-supported textures and, in

Z2C/2 and Z2C/3, they are overlain by rocks of the middle-ramp, offshore facies association, RK2 (typically ribbon-rocks).

DESCRIPTION OF THE EXPOSURE AT MARSDEN BAY

Marsden Bay near Sunderland (Fig. 2) is where the thickest and most complete succession of Z2C slope-apron facies is well-exposed (Fig. 3). However, the base of the Roker Formation (as elsewhere throughout most of its outcrop) is marked by a unit of collapse breccia, formed as a result of dissolution of the underlying Hartlepool Anhydrite. The collapse breccia has a roughly stratiform geometry and is affected by severe diagenetic alteration. In the vicinity of Marsden Bay it is up to 12 m thick but it is possibly only *ca* 3 m thick below the base of the studied section (where it is not exposed). For obvious reasons, the stratigraphy of this part of the section (and therefore the cyclicity within it) cannot be established.

The exposure at Marsden Bay comprises the first two (Z2C/1 and Z2C/2) of the three smaller-scale packages that constitute the Roker Formation (Figs 3, 5 and 11). The criteria used to identify the two packages include the arrangement of the turbidites discussed in this paper. Each consists of lithotypes belonging to facies associations RK1 (slope-apron) and RK2 (offshore/middle-ramp) (Table 1). Only *ca* 45 m of stratigraphy out of a total of *ca* 70 m exposed is examined in this study; this is composed predominantly of lower slope-apron facies.

Z2C/1 is at least *ca* 31 m thick, of which 3 m of collapse breccia in the lowest part cannot be used for thickness studies; its base coincides with that of the Roker Formation. Probably, including most of the collapse breccia, it is composed entirely of lower slope-apron facies. Z2C/1 contains four thick 'slump-sheets', the first (and thickest) just above the collapse breccia unit.

Z2C/2 is at least 37 m thick, of which only the lowest 17 m can be studied; its top is not exposed. The first *ca* 14 m of Z2C/2 consists of lower slope-apron facies; this grades upwards into middle and upper slope-apron facies (*ca* 13 m thick) which, in turn, is overlain by upper slope-apron/outer ramp facies (*ca* 10 m thick). Except for the first *ca* 3 m of the middle-slope facies, cyclicity above the lower slope-apron facies in Z2C/2 cannot be resolved. The failure to resolve this is due to the poor quality of the exposure, facies differences and also because much of the stratigraphy is affected by pervasive soft-sediment deformation and contains a number of syn-sedimentary slide surfaces and faults.

The boundary between Z2C/1 and Z2C/2 is marked by a *ca* 45 cm thick package that contains turbidites and units of laminated lithology which have a high terrigenous clay content. This unit, which is called the 'Orange Marker' because of its distinctive colour, also weathers recessively and so is easily recognizable (Fig. 6). It is also exposed at one other locality in the Sunderland area (Hendon, *ca* 10 km south from Marsden Bay) and, therefore, it can be assumed to be laterally extensive.

DESCRIPTION AND INTERPRETATION OF CYCLICITY

The plots for turbidite thickness, turbidite relative proportion (percentage), turbidite frequency and net rate of accumulation reveal a high degree of organization and cyclicity, with strong regularity (Figs 11, 12A, 12B and 13). For clarity, only turbidites ≥1 cm thick are plotted unless stated otherwise. Analysis of the data reveals up to four orders of cyclicity. These cycles are interpreted below as being Milankovitch-band *ca* 100 kyr short-eccentricity, *ca* 20 and 10 kyr precession and semi-precession cycles and sub-Milankovitch, millennial-scale cycles. Each cycle, at all scales, consists of two parts: a lower part of upward-decreasing trend and an upper part of upward-increasing trend in bed thickness and turbidite percentage. However, as the different types of data set do not correspond exactly to the same stratigraphic units, figures deduced for the thickness and duration of cycles do vary and are thus only approximate. These figures are quoted as thickness (m) from the base of the studied section which, as noted previously, coincides with the top of the collapse breccia, the base of which is the actual base of the Roker Formation itself. In addition to the trends of turbidite bed thickness, percentage and other parameters, compositional criteria were also used to interpret the packaging.

Milankovitch-band cycles

ca 100 kyr short-eccentricity cycles

The largest-scale, longest-duration periodicity present is thought to be the product of a Milankovitch-band short-eccentricity signal of *ca*

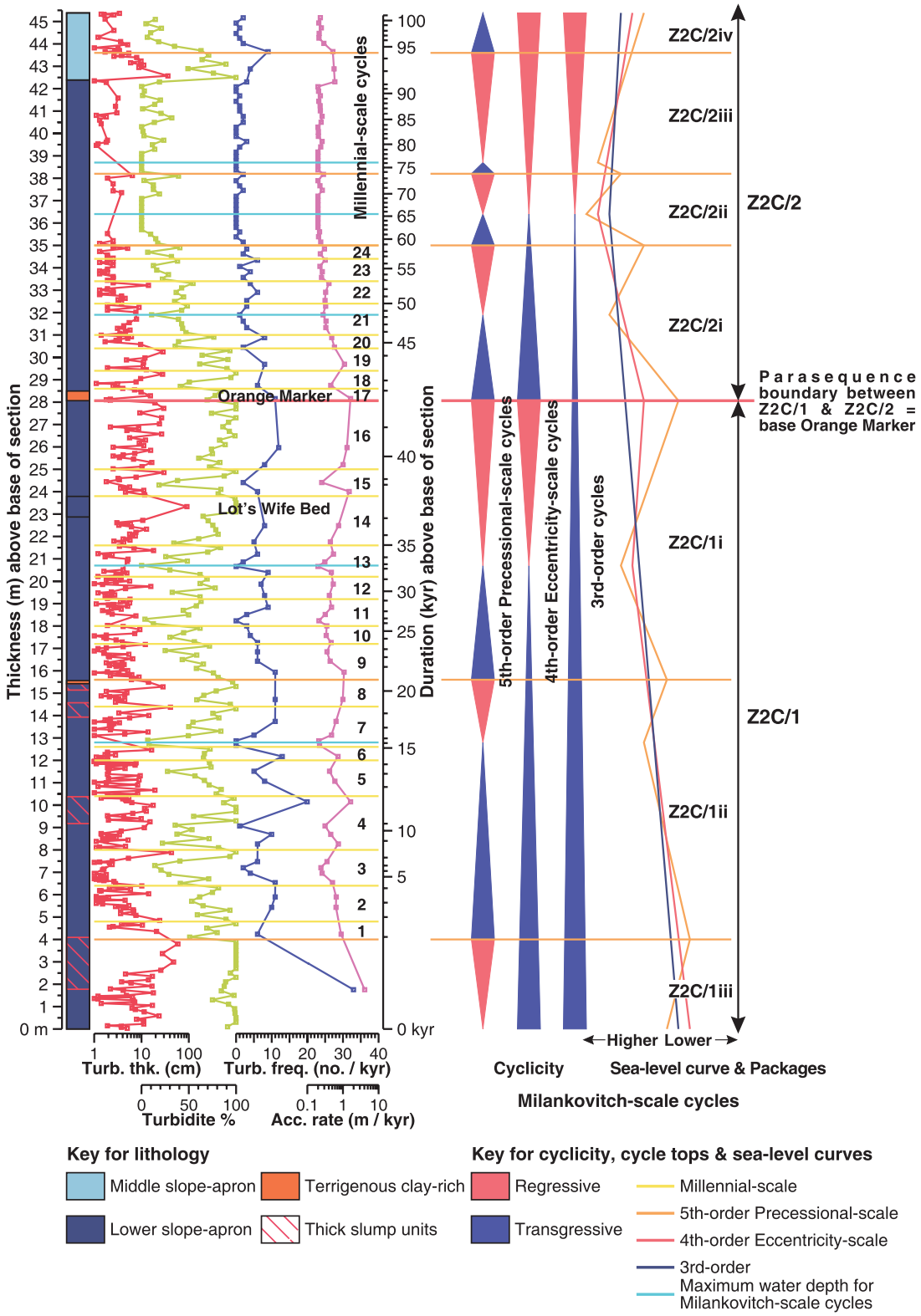

Fig. 11. Plot of turbidite bed thickness (cm, red) and turbidite percentage (% in 20 cm of section, green), turbidite frequency (no. beds per kyr, i.e. within 20 cm of laminated lime-mudstone, blue), and net accumulation rate (cm kyr^{-1}, purple). The left-hand scale is thickness above base of the measured section; the right-hand scale shows the calculated time. The numbers of the millennial-scale cycles are shown (1 to 24, tops marked by yellow lines), The base of the Orange Marker (red line) is taken as a parasequence boundary between the first two (Z2C/1 and Z2C/2) of the three short-eccentricity cycles that constitute the Roker Formation. Tops of precession cycles (Z2C/1i–iii and Z2C/2i–iii) are marked by thin orange lines.

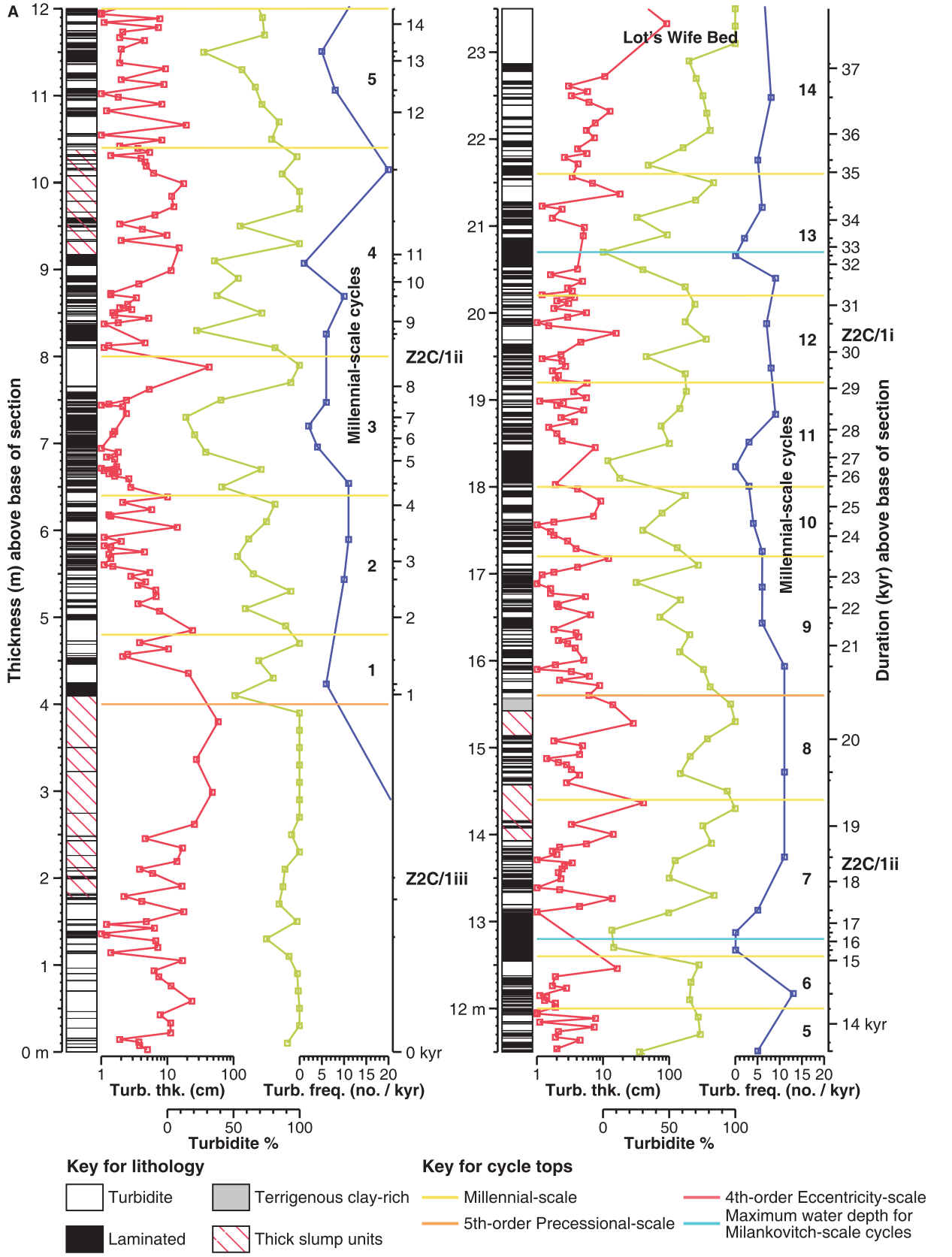

Fig. 12. (A) and (B) Detail of Fig. 11 showing turbidite thickness, frequency and percentage through the succession. Cycle top colours as in Fig. 11. Millennial-scale cycles shown here are numbers 8 to 24.

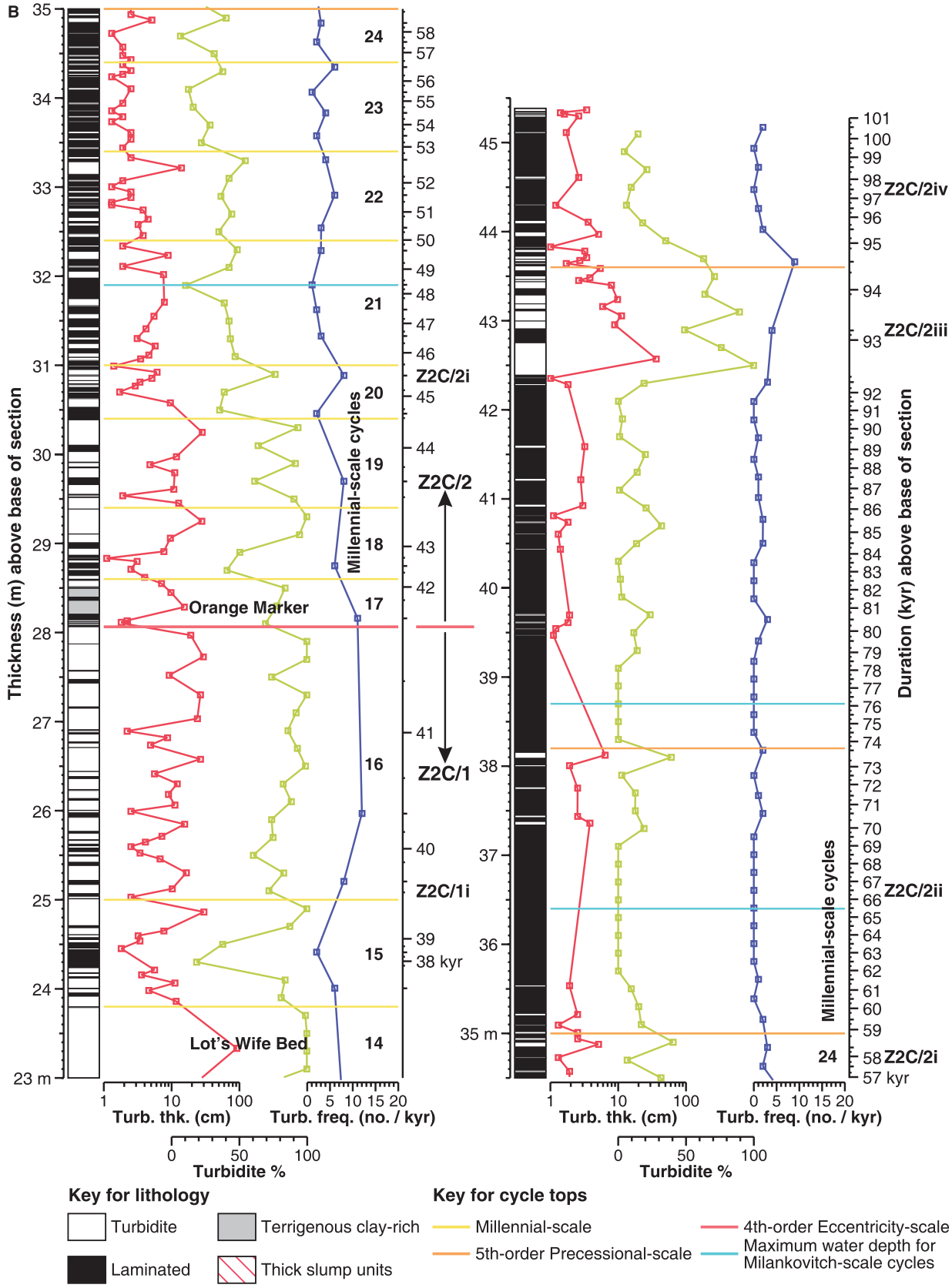

Fig. 12. (Continued).

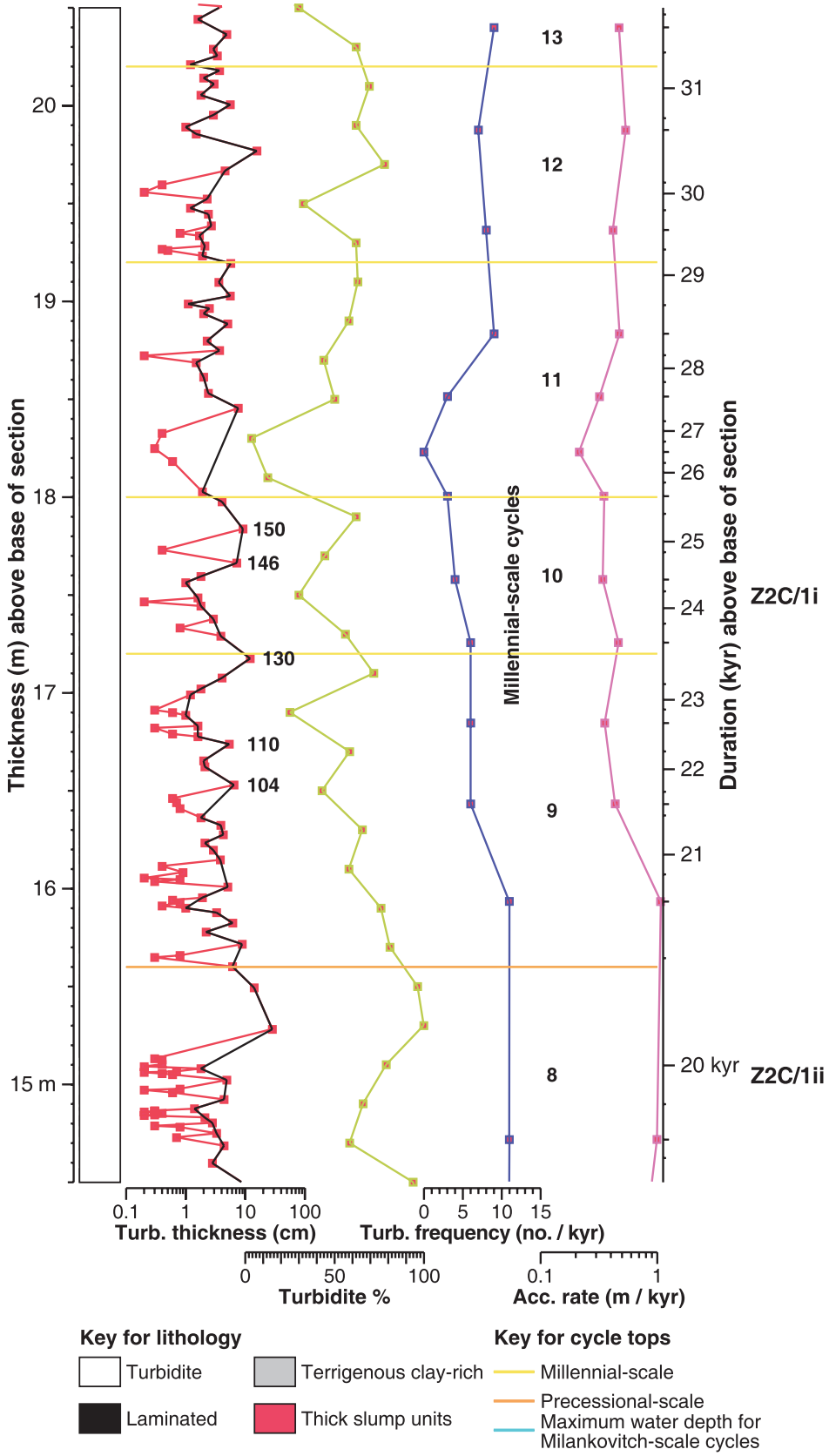

Fig. 13. Detail of Fig. 12 showing millennial-scale cycles 8 to 13, from 14·5 to 20·5 m above base of section. Bed numbers are the same as those indicated on Fig. 7. In the first plot, all turbidites recorded are plotted in red; black lines indicate turbidites ≥1 cm thick.

100 kyr duration. Parts of two such cycles are present in the studied section, represented by Z2C/1 below the Orange Marker and Z2C/2 above. These two packages can be distinguished easily by a very marked change in the packaging of the turbidite beds which occurs around the horizon of the Orange Marker at *ca* 28·1 m. Above the Orange Marker, a pronounced upward decrease in turbidite bed thickness and percentage is seen (Figs 3, 11 and 12B), which is particularly evident in the field. In contrast, the unit immediately below the Orange Marker contains many thick turbidites (including the Lot's Wife Bed) and has a high turbidite percentage (Figs 11 and 12B). These differences are reflected by gross values for turbidite percentage, turbidite frequency and net sediment accumulation rates which, below the Orange Marker (in Z2C/1), are much higher (*ca* 70·5%, one per 138 years and 0·68 m kyr^{-1}, respectively) than those above (in Z2C/2) from which equivalent figures are significantly lower (31%, one per 528 years and 0·29 m kyr^{-1}, respectively). There is less difference in average turbidite bed thickness in Z2C/1 and Z2C/2 (4·1 and 3·5 cm, respectively, for all turbidites). These gross figures consist of data obtained from only the parts of Z2C/1 and Z2C/2 included in the studied section, not the whole of Z2C/1 and Z2C/2.

In detail, each of the two packages comprises two parts, both consisting of upward-decreasing (lower) followed by upward-increasing (upper) trends of turbidite bed thickness, percentage, frequency and rate of sedimentation. The values for all these parameters are consistently high in the first *ca* 16 m of Z2C/1; turbidite frequency (one per 30 years) and net rates of sedimentation (4·1 m kyr^{-1}), in fact, reach their maxima for the entire study section in this unit. These figures are, however, misleading because they include data from all four of the thick slump-sheets in the section and, for reasons given before, turbidite percentage and, to a much greater extent, net rates of sediment accumulation, probably are exaggerated. In addition, it should be noted that the duration of this part of the section is probably slightly greater (by <2 kyr) than indicated and, therefore, actual rates of sedimentation will be reduced; this is because it contains *ca* 40 cm of the clay-rich laminated lithotype (L2) in which the laminae are generally much thinner (*ca* 100 μm) than in L1 (Table 3).

Interestingly, many of the turbidite beds in the lowest 6 m of Z2C/1 contain ooids and are wackestone to packstone textured; above this, ooids are rare and most beds consist largely of lime-mudstone. From *ca* 16 m, all values (turbidite percentage, etc.) show a broad decrease with minima in all reached at 20·7 m, above which upward-increasing trends are seen, up to and including the Orange Marker. Above the Orange Marker, in Z2C/2, all values decrease steadily until reaching a minimum at 36·4 m, above which they show an overall increase in the top *ca* 8 m of the section. Similar trends are also seen in the smaller-scale cycles, described below.

The thickness and duration for the parts of Z2C/1 and Z2C/2 included in the studied section are 28·1 m and 41·4 kyr and 17·3 m and 59·7 kyr, respectively. The total duration of each package can be established by estimating the time represented by the parts of each not included (3 to 12 m of collapse breccia at the base of Z2C/1, *ca* 20 m of middle and upper slope-apron to outer-ramp facies at the top of Z2C/2). A simple calculation using an average sedimentation rate for the whole of the section (*ca* 0·45 m kyr^{-1}) yields a total duration of *ca* 48 to 68 kyr for Z2C/1 and *ca* 104 kyr for Z2C/2. These figures are higher than expected for a *ca* 41 kyr obliquity signal. The relatively low palaeolatitude (*ca* 20°N) of the study area in Late Permian times also suggests that obliquity, which has more of an effect at higher latitudes, is unlikely to have been the cause of this cyclicity (De Boer & Smith, 1994; House, 1995). There is no other indication of an obliquity signal in the data. Consequently, if there is an orbital-forcing control for these larger packages, it could be the *ca* 100 kyr short-eccentricity. An explanation for the apparently short duration (as little as 48 kyr) of Z2C/1 is given in the discussion.

ca 20 kyr precession cycles

The next order of periodicity present is ascribed to Milankovitch-band precession cycles of *ca* 20 kyr duration. These cycles are more strongly developed in Z2C/1 than in Z2C/2; they are distinguished by their *ca* 20 kyr periodicity, which is roughly the same as the duration of *ca* 19·4 kyr predicted for precession cycles in the Permian (De Boer & Smith, 1994). As the base of the studied section does not coincide with that of the Roker Formation, the Orange Marker is used as a datum to identify a total of seven precession cycles, three in Z2C/1 (Z2C/1i to iii) and four in Z2C/2 (Z2C/2i to iv) (Figs 11, 12A and 12B). The cycles in Z2C/1 are numbered downwards from the Orange Marker, those in Z2C/2 upwards from it. Z2C/1iii and Z2C/2iv are incomplete and occur at the very base and very top of the studied

section, respectively; they are not discussed any further. Three of the complete cycles (Z2C/1ii, Z2C/1i and Z2C/2iii) have durations (19·3, 21·2 and 20·7 kyr, respectively) similar to the predicted value of 19·4 kyr. The duration as well as the thickness of both Z2C/2i (17·5 kyr and 6·9 m) and Z2C/2ii (14·7 kyr and *ca* 3·2 m) are probably greater than indicated as it was from this part of the section that thickness data were obtained partly from field photographs. Assuming a duration of *ca* 20 kyr for each cycle, the mis-measured (missing) thickness of laminated lithotype in Z2C/2i and Z2C/2ii is probably *ca* 0·5 and *ca* 1·1 m, respectively. The actual thicknesses of Z2C/2i and Z2C/2ii are therefore at least 7·4 and 4·3 m, respectively.

The cycles display varying degrees of symmetry, Z2C/1ii and, more especially, Z2C/2iii displaying marked asymmetry. The two complete cycles in Z2C/1 are thicker than the three in Z2C/2: Z2C/1i and ii are 12·5 m and 11·6 m thick, respectively, and Z2C/2i, ii and iii, are 6·9 m, 3·2 m and 5·4 m thick, respectively (Fig. 11).

Significantly, a compositional signal is evident in both Z2C/1ii and Z2C/1i and helps to validate their identification. The top half of Z2C/1ii contains a few thicker laminae (2 mm) of orange terrigenous clay and its top is marked by a turbidite bed which, similar to the turbidites in the Orange Marker, contains much disseminated terrigenous clay, giving it a distinctive pink-orange colour. A number of other turbidites in the top half of Z2C/1ii, including one prominent unit which is up to *ca* 64 cm thick and is affected by soft-sediment deformation, contain relatively coarser-grained material (probably ooids and lithic fragments); they have a packstone to wackestone fabric. Two turbidites in the top half of Z2C/1i, including the Lot's Wife Bed (top at *ca* 23·8 m) also contain similar coarser-grained sediment.

ca 10 kyr semi-precession cycles ('half P-cycles')

A relatively strong periodicity of *ca* 10 kyr can be identified within at least two (Z2C/1i and Z2C/1ii) of the four complete precession cycles described above (see Figs 12A, 12B and 13). Each of the precession cycles in these two cycles can be divided into two parts of *ca* 8·6 to 10·9 kyr duration which are interpreted as being the product of semi-precession periodicity, herein referred to as 'half P-cycles'. The four cycles identified are 4·6 to 7·9 m thick and display varying degrees of symmetry. The cycles are fairly symmetric in terms of thickness but more asymmetric with respect to time, the second intervals in three of the four half P-cycles being of shorter duration than their first intervals.

Millennial-scale cycles

Higher-frequency cycles of sub-Milankovitch periodicity are the building blocks of this slope-apron succession. These short-period cycles are best discerned in Z2C/1i, Z2C/1ii and Z2C/2i in which at least 24 cycles (numbered 1 to 24) are recognized (Figs 11, 12A, 12B and 13); they have an average duration of 2·4 kyr with a range of 0·7 to 4·3 kyr (Fig. 14, Table 4). It is not impossible that some of the longer, *ca* 4 kyr cycles are actually two cycles amalgamated. The millennial-scale cycles can be best identified by trends of turbidite bed thickness and percentage which generally display the same polarity and show good correlation; they are not particularly well-resolved by the other data.

The millennial-scale cycles display systematic variations in turbidite bed thickness and percentage and (less strongly) degree of symmetry, which is typical also of the longer-duration cyclicity. In Z2C/1i, Z2C/1ii and Z2C/2i there appear to be eight of the millennial cycles in each (Fig. 11). Like the precession cycles and semi-precession half P-cycles, the millennial-scale cycles are defined best in Z2C/1 and generally are discerned less easily in Z2C/2. The cycles are mostly 0·5 to 1·6 m thick with an average of 1·3 m; one (at the top of Z2C/1, immediately below the Orange Marker) is 3·1 m thick.

The time-scales of the millennial-scale cycles are comparable with the high-frequency cyclicity reported in many Quaternary records. In particular, those of the shorter duration could be equivalent to Dansgaard-Oeschger (*ca* 1470 years) cycles recorded in ice cores (see later *Significance and Discussion* section).

INTERPRETATION AND FORCING MECHANISMS OF CYCLICITY

Although many factors are probably involved, the cyclicity described in this paper records changes in the flux of carbonate to the slope-apron. There are two major factors involved in this process: carbonate productivity and transport 'efficiency' (number and magnitude of shedding events) of sediment from the platform-top to the slope-apron (Roth & Reijmer, 2005). These, in turn, are probably controlled by

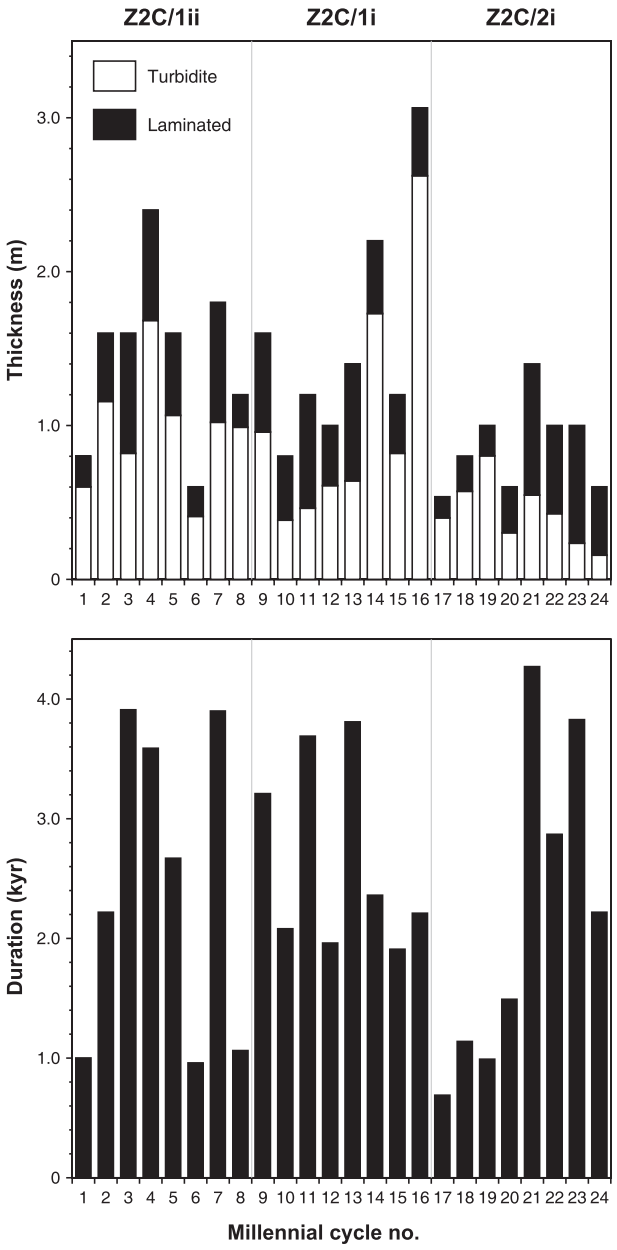

Fig. 14. Histograms showing thickness (m) and duration (kyr) of the millennial-scale cycles. Numbers of cycles (*x*-axes) are as given in Figs 11, 12 and 13 and Table 4.

Table 4. Details of millennial-scale cycles in Z2C/1i, Z2C/1ii and Z2C/2i.

Cycle number	Thickness (m)	Duration (kyr)	Top (m)	Top (kyr)
Z2C/1ii				
1	0.80	1.00	4.80	1.91
2	1.60	2.22	6.40	4.13
3	1.60	3.91	8.00	8.04
4	2.40	3.59	10.40	11.62
5	1.60	2.67	12.00	14.29
6	0.60	0.96	12.60	15.25
7	1.80	3.90	14.40	19.15
8	1.20	1.06	15.60	20.21
Z2C/1i				
9	1.60	3.21	17.20	23.42
10	0.80	2.08	18.00	25.49
11	1.20	3.69	19.20	29.18
12	1.00	1.96	20.20	31.14
13	1.40	3.81	21.60	34.95
14	2.20	2.36	23.80	37.31
15	1.20	1.91	25.00	39.22
16	3.06	2.21	28.06	41.42
Z2C/2i				
17	0.54	0.69	28.60	42.11
18	0.80	1.14	29.40	43.25
19	1.00	0.99	30.40	44.24
20	0.60	1.49	31.00	45.73
21	1.40	4.27	32.40	49.99
22	1.00	2.87	33.40	52.86
23	1.00	3.83	34.40	56.69
24	0.60	2.22	35.00	58.91

relative sea-level and/or a variety of environmental, climatic and oceanographic changes forced by fluctuations of solar irradiance, either related directly to variations in solar output (that is solar forcing) or to changes in the orbit of the Earth (that is orbital forcing).

ca 100 kyr short-eccentricity cycles

The larger-scale packaging of the turbidites seen in Z2C/1 and Z2C/2, thought to be the product of a *ca* 100 kyr short-eccentricity signal, is interpreted through the concept of 'highstand shedding' (Schlager *et al.*, 1994). Accordingly, the primary control that produced them is believed to have been changes in relative sea-level which, in turn, affected carbonate productivity. Environmental factors such as water temperature and climate may well have played a part too but are considered to have been subordinate to the changes caused by relative sea-level. In the context of 'highstand shedding', Z2C/1 and Z2C/2 are each considered to be transgressive to regressive packages. Trends of upward-decreasing turbidite bed thickness, percentage, frequency and rates of accumulation are considered to mark periods of transgression; trends of upward-increasing turbidite thickness, percentage, frequency and rates of accumulation are considered to mark periods of highstand. Relatively thick units of the laminated lithotype are thought to mark periods of maximum water depth and, in terms of sequence stratigraphy, therefore, to represent the maximum flooding 'surface' (MFS) of each package. Interestingly, concentra-

tions of fossil fish occur in the laminated lithotype at two localities, one of which is the MFS interval of Z2C/2 at Marsden Bay (Kirkby, 1863, 1864; Howse, 1880). Similar packaging of turbidites has been recorded in Quaternary strata by Kuhn & Meischner (1988), Schlager *et al.* (1994) and Bernet *et al.* (2000).

The relative sea-level rise associated with Z2C/2 might have been greater than that for Z2C/1 because the MFS interval for Z2C/2 is much thicker and of longer duration (*ca* 1·8 m, 9 kyr) than in Z2C/1 (*ca* 0·3 m, 1·7 kyr). This interpretation is substantiated by the much lower values in Z2C/2 relative to Z2C/1 for average turbidite bed percentage (31%, 70·5%) and frequency (528 years, 138 years), and net rates of accumulation (0·29 m kyr^{-1}, 0·68 m kyr^{-1}) quoted previously. Z2C/1 is markedly asymmetric in terms of duration and thickness (Fig. 11). The MFS interval for Z2C/1 is located at 20·7 m (32·7 kyr) from the base of the study section or 47·1 m (91·3 kyr) above the base of Z2C/1 (equivalent to the base of the Z2C) because, as discussed later, the original thickness of the collapse breccia was probably 26·4 m (20·7 + 26·4 = 47·1 m). Assuming a duration of *ca* 100 kyr for Z2C/1, the MFS interval is located 8·7 kyr below its top, which gives 91·3 kyr from its base. The transgression associated with Z2C/1 was, therefore, of longer duration and also relatively slow, because relatively high carbonate production on the platform was maintained throughout most of this period.

The initial transgression associated with Z2C/1 appears to have coincided with the end of evaporite precipitation (which deposited the Hartlepool Anhydrite) and the start-up of carbonate production (which deposited the Roker Formation). Thus the contact between the Hartlepool Anhydrite and Roker Formation does represent a significant stratigraphic boundary but it does occur within the early transgressive part of the third-order sequence which constitutes the Roker platform as a whole. As turbidites containing ooids and units of the clay-rich laminated lithotype (L2) are common in this lower transgressive part of Z2C/1, but are rare or absent above, it is probable that water depths during the early stages of the transgression were less than those existing during the subsequent highstand period. Rates of carbonate production in this TST were thus able to keep up with the rise of relative sea-level.

Z2C/2 is also asymmetric in terms of time and thickness (significantly less so in terms of time); the MFS is located at 8·3 m (24·1 kyr) above its base and, therefore, 28·7 m of stratigraphy occurs above it (Fig. 11). Unlike Z2C/1, therefore, it is predominantly regressive in character although most of the section studied belongs to the transgressive part. As noted above, the relative sea-level rise associated with Z2C/2 was of greater magnitude than that associated with Z2C/1. This fact is also substantiated by facies analysis at other localities in the region which indicates that this is the MFS interval for the Roker Formation sequence as a whole. The transgression was also clearly much more rapid than in Z2C/1 because, in Z2C/2, it lasted for a period of *ca* 24 kyr, when compared with *ca* 91 kyr in Z2C/1. Initially, rates of sea-level rise must have been slow enough to allow relatively high carbonate productivity because the first 2·5 m of Z2C/2 has a relatively high percentage of turbidites. As an alternative, this material may have been reworked from sediment produced during the previous highstand. The change from transgressive to highstand conditions in Z2C/2 appears to have coincided with platform/slope-apron progradation, because *ca* 3 m above the MFS interval, the transition from lower to middle slope-apron facies begins.

The Orange Marker (Figs 6 and 11) is thought to represent a relative sea-level fall and to mark the boundary between Z2C/1 and Z2C/2 on the basis of the pronounced change in the style of packaging associated with it, together with its relatively high terrigenous clay content. This increase in the flux of clastic material is characteristic of many carbonate systems during periods of forced regression and lowstand (Hunt & Tucker, 1993; Southgate *et al.*, 1993; Tucker, 2003b). As there is no evidence of exposure associated with this unit, the placement of a parasequence boundary at the base of the Orange Marker may seem rather arbitrary; however, the turbidite percentage and frequency seem to substantiate this interpretation. This view follows that of the Grant *et al.* (1999) sequence stratigraphic interpretation of pelagic chalk facies and other carbonate sequence stratigraphic models (references above and also Emery & Myers, 1996; Coe *et al.*, 2003) which place the sequence boundary where the first evidence for relative sea-level fall is found. The boundary here in reality then is the correlative conformity, as well as the basal surface of forced regression in the scheme of Hunt & Tucker (1992). Sequence stratigraphic terminology is reviewed in Catuneanu *et al.*, 2009.

The small thickness of the falling-stage/lowstand part of the section (*ca* 45 cm), represented

by the Orange Marker, is another feature typical of carbonate systems because mechanical reworking of carbonate rocks on the exposed platform is generally limited by their early lithification. Another contributing factor, which is equally important, and which may also explain the fine nature of the clastics in the Orange Marker, was the arid climate during Roker Formation times. This climate probably inhibited mechanical reworking and transport of terrigenous sediments; much of the clay is possibly aeolian in origin. At the correlative horizon on the platform-top, there is no obvious exposure surface and clastic influx is seen at only one locality (Hawthorn Quarry). The general lack of evidence for exposure is probably due to a combination of erosion and, more probably, the fact that such surfaces are usually poorly developed in hot, arid environments, such as those existing during the Zechstein. However, Strohmenger *et al.* (1996a) have described karstic exposure horizons in the Z2C of Germany.

ca 20 kyr precession cycles

In view of their duration, the most important control of the *ca* 20 kyr precession cycles is also thought to be changes in carbonate productivity caused by changes of relative sea-level and associated environmental changes, and their packaging is interpreted accordingly. Evidence for sea-level fluctuations of this duration is observed in many Quaternary coral-reef records (Fairbanks, 1989) and they are commonly interpreted as being the cause of shallowing-upward cycles (parasequences) in a wide range of settings and sedimentary rock-types throughout the geological record (Lehrmann & Goldhammer, 1999 and papers cited previously). The occurrence of coarser-grained turbidites and clastics at the top of two of the cycles also supports this interpretation. A compositional signal such as this is, in fact, predicted by highstand shedding models (Schlager, 1992) and is documented from slope facies throughout the geological record as, for example, in the Triassic (Reijmer *et al.*, 1994), Cretaceous (Hunt & Tucker, 1993) and many examples from the Quaternary (see references given previously).

ca 10 kyr semi-precession cycles ('half P-cycles')

The interpretation of these cycles is not clear but, given their duration, their forcing mechanism, similar to the *ca* 20 kyr precession cycles, is probably associated with the relative sea-level changes. Reuning *et al.* (2006) have documented half-precession cycles in aragonite content data from slope carbonates of the Bahamas.

Millennial-scale cycles

These relatively short-period cycles are perhaps the most interesting of all the cycles present and their interpretation is controversial. Relative sea-level change is a possibility, although it would be at a much higher frequency than the Milankovitch rhythms. Sub-Milankovitch sea-level cycles have been inferred from Pleistocene oxygen isotope data (Thompson & Goldstein, 2005; Rohling *et al.*, 2007) but this was an icehouse time, contrasting with the Upper Permian probable ice-house to green-house transitional state, when any sea-level changes would have been subdued through much reduced or absent polar ice-caps. More probable controls are fluctuations in climate and/or environmental factors affecting carbonate productivity and/or sediment supply. For example, carbonate productivity could have been increased through higher sea water temperature and/or aridity, thus increasing the size of the sediment 'reservoir' on the platform-top. The volume (flux) of carbonate sediment transported from the reservoir to the slope could have fluctuated as well. For instance, regional changes of climate could have increased storm intensity and frequency, or simply raised fair-weather wave-height and wave-energy so that 'shedding-events' (turbidity currents and hyperpycnal flows) were more frequent and of greater magnitude.

Short-term climatic and oceanographic changes have been recognized relatively recently in a wide variety of Quaternary records (Bond *et al.*, 1997, 2001; Dansgaard *et al.*, 1993; GRIP, 1993; Hughen *et al.*, 1996a,b; Johnsen *et al.*, 1992; Schulz *et al.*, 1998; Yancheva *et al.*, 2007). The *ca* 1500 year Dansgaard-Oeschger cycles are particularly relevant as they are the result of sharp warming events followed by cooling. If the millennial-scale cycles were driven by climate change, then some other parameter must have been fluctuating to change climate on this high-frequency scale. The most probable explanation then is fluctuations in solar output, as suggested by many of the above-cited papers; and, in this context, of particular interest is the deduction that the duration of the millennial-scale cycles recognized here does not appear to have been equal, only quasi-periodic or non-canonical. As shown in Table 4 and Fig. 14, the

durations vary from *ca* 700 to *ca* 4300 years (although some of the longer-duration cycles could be amalgamated). Note also that there is a suggestion of increasing and decreasing durations.

It has been suggested, however (Foukal *et al.*, 2006), that there is ''no evidence for solar luminosity variations of sufficient amplitude to drive significant climate variations on centennial, millennial and even million-year timescales''. This suggestion leaves only one other potential mechanism for quasi-regular changes in climate – major changes in volcanic activity. Ward (2009) has presented strong arguments that high rates of SO_2 emission from volcanic activity (i.e. more than one large volcanic eruption each year for decades) will lead to global warming. Ward demonstrated that the millennial-scale sharp warming events of the last *ca* 50 000 years, the Dansgaard-Oeschger cycles, were contemporaneous with times of major volcanic eruptions. Thus, the arguments continue regarding the ultimate driving mechanisms for short-term and long-term climate change; however, this does not devalue the sedimentological record in any way, where the evidence for such changes is often so well-preserved.

OTHER EXPLANATIONS FOR THE PACKAGING

There are other processes that could be invoked for the packaging of the turbidites, other than sea-level and climate change affecting carbonate productivity and sediment transport, but most of these alternatives can be discounted on the grounds of the high degree of organization and periodicity shown by the cyclicity. It could be argued, for example, that the packages, especially the smaller-scale, higher-frequency cycles, were produced by random variations in turbidite bed thickness (see Hiscott, 1981 for discussion). The fact that these cycles are apparently so well-organized and display such a strong periodicity suggests that they are real. Statistical tests and other analytical approaches (Murray *et al.*, 1996), especially for the millennial-scale cycles, could confirm their existence for sceptics of the data and interpretations presented here; however, the apparent quasi-periodic nature of the millennial-scale cycles (see Fig. 14, Table 4) may make it impossible to identify them through spectral analysis.

A tectonic control could be invoked for the packaging. For instance, it could be argued that the larger-scale packages (Z2C/1 and Z2C/2) were generated by syn-sedimentary, fault-related uplift. There is evidence at Marsden Bay for such tectonic activity. This evidence includes thickness and facies changes across a fault (located near Smuggler's Cave; see Fig. 2) and also the facing directions of slump-folds in Z2C/2, which are strongly oblique to the general north-east facing (basinward) direction of the slope-apron. However, the fact that Z2C/1 and Z2C/2 can be recognized throughout the outcrop of the Roker Formation (and also probably throughout the Zechstein Basin), indicates that they were caused by basin-wide, not local, changes of relative sea-level. The strong periodicity of the *ca* 20 kyr-scale and millennial-scale cycles indicates that a tectonic origin for them is unlikely. Some of the thicker turbidites, such as the Lot's Wife Bed, may have been triggered by fault movement, however.

It is also possible that the larger-scale trends of upward-increasing turbidite bed thickness and percentage could have been caused by platform progradation. This effect is, however, unlikely given that the laminated lithology is almost entirely of the same type (L1) throughout all of Z2C/1 and most of Z2C/2; this suggests that the depositional setting throughout most of Z2C/1 and Z2C/2 times at Marsden Bay remained broadly the same. The relatively thickly laminated lithotype (L3), which is just found in middle slope-apron facies, occurs only at the top of the section at Marsden Bay. A progradation explanation also fails to explain how the larger-scale trends of upward-decreasing turbidite thickness and percentage could have been generated; platform retreat would require an external forcing mechanism such as a relative sea-level rise and/or environmentally related inhibition of carbonate productivity.

A number of deep-water sedimentary processes could explain some of the packaging (see Pickering *et al.*, 1989; Stow *et al.*, 1996). For example, channel and/or lobe migration, switching and abandonment provide possible explanations for the upward increasing/decreasing patterns of turbidite bed thickness. Thick, massive units in the upper and middle slope-apron at Marsden Bay may occupy channels but channellization is not observed at all in the lower slope-apron facies. The lack of scouring and the mud-rich nature of most of the turbidite beds also suggest that channellization associated with their deposition is unlikely to have occurred. The interpretation of the packages as lobe sheets is harder to

discount, however, especially given the uncertainty regarding the size of such features and the general paucity and limited extent of exposures of the Roker Formation in the region. Sedimentary processes associated with lobe sheets could also have produced the smaller-scale thickening and thinning-up packages (so-called 'compensation cycles'; Hiscott, 1981; Stow *et al.*, 1996) but significant lateral thickness changes are not discernible in the turbidite beds and so this explanation is also considered unlikely. Taking all the data into account, the well-organized nature and strong periodicity of the cycles suggest that purely sedimentary processes are unlikely to have generated the packaging.

VALIDITY OF THE TIME-SCALE

The validity of the time-scale used in this study is critical for the interpretation of the cyclicity. In particular, the assumptions made regarding the annual origin of the laminae and their uniform thickness are clearly open to question. The time-scale can be tested, however, by comparing the data with those from modern examples and the rest of the geological record. Such a comparison indicates that the time-periods suggested here for the cycles are reasonable. For example, the net rate of accumulation for the whole of the studied section is *ca* 0·45 m kyr^{-1} which, although higher than the average for the sedimentary record (see data in Schlager, 1992), is geologically realistic when compared with Quaternary data. Equivalent figures for just the parts of Z2C/1 and Z2C/2 included in this study are 0·68 and 0·29 m kyr^{-1}, respectively. The same figures for the five complete precession cycles in the study section (Z2C/1i and ii and Z2C/2i to iii) vary between *ca* 0·2 and *ca* 0·6 m kyr^{-1}. Data from eight of the 1000 year time-slices show figures >1 m kyr^{-1} of which six are between 1 and 1·5 m kyr^{-1}. The two highest values (*ca* 4·1 and *ca* 1·6 m kyr^{-1}) occur in time-slices at the base of the section that each contain one of the two very thick slump-sheets and, for reasons given earlier, probably are unreliable. The data generated in this study also produce realistic values for net rates of accumulation of the Roker Formation as a whole (see *Significance and Discussion*). Note that any comparison of the net rate of sedimentation for the Roker Formation with modern data must take into account the fact that the data derived from this study are for compacted sediment and, therefore, will have originally been higher than indicated above. Decompacted thicknesses are calculated to be *ca* 20% to 30% higher if a maximum burial depth of 1 to 2 km is assumed for the Roker Formation.

Turbidite frequency data also give realistic results. The average frequency of all turbidites in the study section is one every *ca* 158 years and one every 244 years for turbidites ≥1·0 cm thick. Figures from both Z2C/1i and Z2C/1ii show an average frequency of one every 170 and 135 years, respectively, for turbidites ≥1·0 cm thick. In Z2C/2i to iii, equivalent figures are much lower, varying from one every 253 to 1637 years for turbidites ≥1·0 cm thick. Many of these figures are comparable with the periodicity of major so-called '100 to 200 year' storm events predicted for the present-day North Sea (Light & Wilson, 1998) and to the frequency of category 5 cyclones (200 to 300 years) for the Great Barrier Reef (Nott & Hayne, 2001). Data from the Bahamas (Tongue of the Ocean, Exuma Sound), however, show that turbidite frequency is an order of magnitude, or more, less than that in the Roker Formation: <1 to 6 per 10 kyr (Droxler & Schlager, 1985; Kuhn & Meischner, 1988; Bernet *et al.*, 2000). Net rates of accumulation are also proportionally less (*ca* 1 to 8 cm kyr^{-1}). These markedly contrasting figures are probably due to fundamental differences in scale between the two systems; the Roker Formation slope-apron was only *ca* 100 m in height whereas the Bahamian slopes have a much higher bathymetric relief of *ca* 1000 m or more. A further factor that must be considered when making comparisons with data from the Quaternary is that production then was associated with major glacio-eustatic sea-level changes, unlike those in the Roker Formation (see later). Shanmugam (2008) demonstrated the significant role of tropical cyclones in transporting sediment from shelves to slopes.

One further point regarding the time-scale is that the duration of 48 to 68 kyr calculated previously for Z2C/1 is too short to be interpreted as a *ca* 100 kyr short-eccentricity signal. These figures included an estimate for the duration of the 3 to 12 m thick unit of collapse breccia at its base by using the average sedimentation rate (0·45 m kyr^{-1}) derived from the entire study section. As there is no evidence for any major stratigraphic break within the collapse breccia, an obvious explanation for the discrepancy is that the actual rate of accumulation for this section was much lower. Assuming a duration of *ca* 100 kyr for Z2C/1, the amount of time represented by this unit would have been *ca* 58·6 kyr

(the duration of the dated part of Z2C/1 is 41·4 kyr) and, therefore, the rate of sedimentation for the collapse-brecciated unit would have been between only 0·05 and 0·2 m kyr^{-1}. As this figure is relatively low for the Roker Formation, an alternative explanation is that the strata now forming the collapse breccia were originally much thicker than at present. This view is suggested because subsurface evidence (cores) shows that, throughout the platform, the bottom part of the Roker Formation contains much anhydrite (displacive and replacive). The removal of this by dissolution would, it is suggested, have significantly reduced the original thickness of these rocks. As the time represented by the collapse breccia is known roughly (58·6 kyr), its original thickness can be determined from the average sedimentation rate of the study section (0·45 m kyr^{-1}), yielding a figure of *ca* 26·4 m for the original thickness of the collapse brecciated unit; i.e. 14·4 to 23·4 m more than it is now. Performing a similar calculation for the top part of Z2C/2 which is not dated (and which would have had a duration of *ca* 40·3 kyr) yields a figure of 18·1 m, comparable with the actual figure of 20 m; this suggests that such an approach is correct. The original thickness of Z2C/1 was therefore *ca* 54·5 m (28·1 + 26·4 = 54·5 m).

SIGNIFICANCE AND DISCUSSION

The importance of this study is that cyclicity of various types can be recognized using turbidite-bed and laminated-mudstone thickness patterns. The packaging of the turbidites is very well-organized and displays a strong periodicity that clearly does not have a random signature. The recognition of the millennial-scale sub-Milankovitch cycles is of particular interest as this demonstrates that such cyclicity can be recognized in the pre-Pleistocene geological record, even when high-resolution biostratigraphic and radiometric data are not available. Significantly, this also indicates that the record of millennial-scale cyclicity could, in fact, be much more widespread in the geological record than considered previously and that it may be recognized by variations of bed thickness in suitable facies (notably shelf carbonates, see Tucker *et al.*, 2009).

The shorter-duration Milankovitch-band and millennial-scale cycles are most strongly defined in the early transgressive and highstand parts of larger, interpreted eccentricity-scale fluctuations of relative sea-level. The signal of this higher-frequency cyclicity therefore is weaker than that associated with the longer-duration/higher-amplitude, eccentricity-scale related changes of relative sea-level, i.e. those recognized as 'highstand-shedding'. The precessional and millennial-scale signal is clearly amplified or muted by the variations in carbonate productivity and supply caused by these longer-term changes.

Eccentricity and precessional-scale changes of relative sea-level are much more significant during icehouse times, such as the Quaternary, through a glacio-eustatic mechanism. The Late Permian, however, was a transitional time following the end of the Gondwanan glaciation (Angiolini *et al.*, 2003; Montañez *et al.*, 2007), leading to the greenhouse conditions of the Triassic. In the Late Permian sea-level changes would have been of lower amplitude than in the Lower Permian, although there may well have been an influence from residual polar ice. Global computer climate modelling (Crowley, 1994; Kutzbach, 1994; Barron & Fawcett, 1995; Gibbs *et al.*, 2002) and floral evidence (Ziegler, 1990a; Rees *et al.*, 1999, 2002) have shown that the climate of the Earth during the Late Permian was significantly warmer (by up to *ca* 6·5 °C) than at present. The Zechstein Basin is thought to have undergone periodic isolation, especially in the latest Permian and at times of evaporite precipitation (Tucker, 1991), but it was most probably connected to the open ocean during times of carbonate deposition.

The arid climate and near-landlocked nature of the Zechstein Sea would have made it particularly sensitive to changes in solar irradiance and global warming events and these may have reinforced even minor sea-level and environmental variations. The strong seasonality of the global climate, also indicated by computer modelling, could also have amplified further even small changes of irradiance caused by orbital and solar forcing (see references above). These factors may explain why the high-frequency millennial-scale signal is so well-recorded in the Roker Formation slope-apron facies. The fact that some of the millennial-scale cyclicity is of broadly similar duration to the *ca* 1500 year periodicity of Dansgaard-Oeschger cycles is especially significant for two reasons, assuming that in both cases the cycles are the product of the same forcing mechanism. Firstly, it suggests that the same process or processes were operating in the Permian as during the Quaternary and, secondly, an explanation for these cycles must exclude one controlled purely

by thermohaline circulation, because, as noted above, the Earth was in a transitional icehouse to greenhouse state in Late Permian times.

Another important result of this study is that it allows the time interval represented by the Roker Formation (Z2C) as a whole to be estimated; this is because the duration of two of the large-scale packages (Z2C/1 and Z2C/2) that constitute the Z2C are probably the product of *ca* 100 kyr short-eccentricity rhythms. As there is a third package of comparable thickness to the first two within Z2C, the duration of the Roker Formation can be inferred to be up to 0·3 Myr. This figure is in broad agreement with the estimate of Menning *et al.* (2005) of 0·8 Myr for the duration of the whole of the second Zechstein cycle, which includes a very thick basin-centre halite, and non-deposition. The duration for the Z2C suggested here contrasts markedly with the estimate of *ca* 1·5 Myr given by Leyrer *et al.* (1999) for the Z2C in Germany. A duration of 0·3 Myr produces net accumulation rates for the Roker Formation of between 0·45 m kyr^{-1} for the slope-apron (maximum thickness *ca* 140 m) and *ca* 0·2 m kyr^{-1} for the platform-top (maximum thickness 60 m). Using a duration of 1·5 Myr for the Roker Formation gives equivalent rates of *ca* 0·1 and *ca* 0·04 m kyr^{-1}, which seem extremely low. If the assumptions are correct, it implies that much of the sediment on the platform-top was exported, because, using an average sedimentation rate of 0·45 m kyr^{-1} for the slope-apron facies at Marsden Bay and a duration of 300 kyr for the Roker Formation, it can be calculated that *ca* 135 m of carbonate sediment would have been produced on the platform-top. Therefore, more than half the sediment produced on the platform-top was probably exported because there is no evidence for significant exposure in the platform-top succession. The high rate of export is partly a reflection of the lack of accommodation space on the platform top itself, along with high carbonate productivity and efficient export processes. As shown by this study, the flux of sediment varied and was strongly cyclic at a range of periodicities including a sub-Milankovitch, millennial-scale frequency, which in this paper is attributed to fluctuations in solar output.

CONCLUSIONS

The lower slope facies of the Upper Permian Roker Formation in North-east England shows a clear hierarchy of cyclicity on scales from metres to tens of metres. The slope cycles basically are defined by the thickness, percentage and frequency of carbonate turbidites interbedded with laminated lime-mudstones, caused by variations in sediment export from the adjacent platform. The control on this will have been fluctuations in carbonate productivity, driven by changes in sea-level, climate and/or environmental factors. The durations of the cycles are from millennial-scale (700 to 4300 years) to Milankovitch-scale (precession, *ca* 20 000 years and short-eccentricity, 100 000 years). The ultimate control on the Milankovitch-scale cycles would have been variations in solar irradiance because of the orbital forcing. However, the origin of the quasi-periodic millennial-scale cycles, likely responses also to climate change, is debateable; variations in solar luminosity or volcanic activity are the two possibilities.

ACKNOWLEDGEMENTS

The authors are grateful to the late Denys Smith for encouragement and discussions during the early stages of this research and to Martin Jones and Mick Jones (both from the University of Newcastle upon Tyne) for providing geochemical data. We also thank Prof. M. Menning for comments on Permian stratgraphy. We acknowledge the most useful comments of the referees, Rainer Zühlke and Christian Strohmenger, and the Assistant Editor, Christian Betzler. MET is grateful to VMT for her tolerance of millennial-scale cycles. MM would like to thank MB for her tolerance as well and for supporting his Ph.D. research.

REFERENCES

Anderson, R.Y. (1982) A long geoclimatic record from the Permian. *J. Geophys. Res.*, **87,** 7285–7294.

Anderson, R.Y. (1996) Seasonal sedimentation: a framework for reconstructing climate and environmental change. In: *Palaeoclimatology and Palaeoceanography from Laminated Sediments* (Ed. A.E.S. Kemp), *Geol. Soc. Spec. Publ.*, **116,** 1–5.

Angiolini, L.L, Balini, M., Garzanti, E., Nicora, A. and **Tintori, A.** (2003) Gondwanan deglaciation and opening of Neotethys: the Al Khlata and Saiwan Formations of Interior Oman. *Palaeogeogr. Palaeoclimatol. Palaeoecol.*, **196,** 99–123.

Bádenas, B., Aurell, M. and **Gröcke, D.R.** (2005) Facies analysis and correlation of high-order sequences in middle-outer ramp successions: variations in exported carbonate on basin-wide $\delta^{13}C_{carb}$ (Kimmeridgian, N.E. Spain). *Sedimentology*, **52,** 1253–1275.

Barron, E.J. and **Fawcett, P.J.** (1995) The climate of Pangaea: a review of climate model simulations of the Permian. In: *The Permian of Northern Pangea* Volume 1 (Eds P.A. Scholle, T.M. Peryt and D.S. Ulmer-Scholle), pp. 37–53. Springer-Verlag, Berlin.

Behl, R.J. and **Kennet, J.P.** (1996) Brief interstadial events in the Santa Barbara basin, NE Pacific, during the past 60 kyr. *Nature*, **379,** 243–246.

Bernet, K.H., Eberli, G.P. and **Gilli, A.** (2000) Turbidite frequency and composition in the distal part of the Bahamas transect. In: *Proceedings of the Ocean Drilling Program, Scientific Results* (Eds P.K. Swart, G.P. Eberli, M.J. Malone and J.F. Sarg), *Ocean Drilling Program*, **166,** 45–60.

Bond, G., Showers, W., Cheseby, M., Lotti, R., Almasi, P., deMenocal, P., Priore, P., Cullen, H., Hajdas, I. and **Bonani, G.** (1997) A pervasive millennial-scale cycle in North Atlantic Holocene and glacial climates. *Science*, **278,** 1257–1266.

Bond, G., Kromer, B., Beer, J., Muscheler, R., Evans, M.N., Showers, W., Hoffmann, S., Lotti-Bond, R., Hajdas, I. and **Bonani, G.** (2001) Persistent solar influence on North Atlantic climate during the Holocene. *Science*, **294,** 2130–2136.

Catuneanu, O., Abreu, V., Bhattacharya, J.P., Blum, M.D., Dalrymple, R.W., Eriksson, P.G., Fielding, C.R., Fisher, W.L., Galloway, W.E., Gibling, M.R., Giles, K.A., Holbrook, J.M., Jordan, R., Kendall, C.G.St.C., Macurda, B., Martinsen, O.J., Miall, A.D., Neal, J.E., Nummedal, D., Pomar, L., Posamentier, H.W., Pratt, B.R., Sarg, J.F., Shanley, K.W., Steel, R.J., Strasser, A., Tucker, M.E. and **Winker, C.** (2009) Towards the standardization of sequence stratigraphy. *Earth-Sci. Rev.*, **92,** 1–33.

Clark, D.N. (1980) The sedimentology of the Zechstein 2 carbonate formation of eastern Drenthe, The Netherlands. In: *The Zechstein Basin with Emphasis on Carbonate Sequences* (Eds H. Füchtbauer and T.M. Peryt), *Contrib. Sedimentol.*, **9,** 131–165.

Clark, D.N. (1986) The distribution of porosity in Zechstein carbonates. In: *Habitat of Palaeozoic Gas in N.W. Europe* (Eds J. Brookes, J.C. Goff and B. van Hoorn), *Geol. Soc. Spec. Publ.*, **23,** 121–149.

Coe, A., Bosence, D., Church, K., Flint, S., Howell, J. and **Wilson, C.** (2003) *The Sedimentary Record of Sea-level Change*. The Open University, Milton Keynes, 285 pp.

Crowley, T.J. (1994) Pangean climates. In: *Pangea: Palaeoclimate, Tectonics, and Sedimentation during Accretion, Zenith, and Breakup of a Supercontinent* (Ed G.D. Klein), *Geol. Soc. Am. Spec. Pap.*, **288,** 25–39.

Dansgaard, W., Johnsen, S.J., Clausen, H.B., Dahl-Jensen, D., Gundestrup, N.S., Hammer, C.U., Hvidberg, C.S., Steffensen, J.P., Sveinbjörnsdottir, A.E., Jouzel, J. and **Bond, G.** (1993) Evidence for general instability of past climate from a 250-kyr ice-core record. *Nature*, **364,** 218–220.

De Boer, P.L. and **Smith, D.G.** (1994) Orbital forcing and cyclic sequences. In: *Orbital Forcing and Cyclic Sequences* (Eds P.L. De Boer and D.G. Smith), *Int. Assoc. Sedimentol. Spec. Publ.*, **19,** 1–14.

Droxler, A.W. and **Schlager, W.** (1985) Glacial versus interglacial sedimentation rates and turbidite frequency in the Bahamas. *Geology*, **13,** 799–802.

Elrick, M. and **Hinnov, L.A.** (1996) Millennial-scale climate origins for stratification in Cambrian and Devonian deep-water rhythmites, western USA. *Palaeogeogr. Palaeoclimatol. Palaeoecol.*, **123,** 353–372.

Elrick, M. and **Hinnov, L.A.** (2007) Millennial-scale paleoclimate cycles recorded in widespread Palaeozoic deeper water rhythmites of North America. *Palaeogeogr. Palaeoclimatol. Palaeoecol.*, **243,** 348–372.

Emery D. and **Myers K.J.** (Eds) (1996) *Sequence Stratigraphy*. Blackwell Science, Oxford, 297 pp.

Fairbanks, R.G. (1989) A 17,000-year glacio-eustatic sea-level record: influence of glacial melting rates on the Younger Dryas event and deep-ocean circulation. *Nature*, **342,** 637–642.

Fensome, C. (2002) Depositional environment, palynofacies and organic geochemistry of the Zechstein Z1 cycle Marl Slate and Z2 cycle Stinkschiefer and Concretionary Limestone: from a study of the W14A and B8 cores. M.Sc. thesis, University of Newcastle upon Tyne, Newcastle upon Tyne, viii + 81 pp.

Foukal, P., Fröhlich, C., Spruit, H. and **Wigley, T.M.L.** (2006) Variations in solar luminosity and their effect on the Earth's climate. *Nature*, **443,** 161–166.

Gibbs, M.T., Rees, P.McA., Kutzbach, J.E., Ziegler, A.M., Behling, P.J. and **Rowley, D.B.** (2002) Simulations of Permian climate and comparisons with climate-sensitive sediments. *J. Geol.*, **110,** 33–55.

Glennie, K.W. (1972) Permian Rotliegendes of northwest Europe intepreted in the light of modern desert sedimentation studies. *Bull. Am. Assoc. Petrol. Geol.*, **56,** 1048–1071.

Glennie, K.W. (1982) Early Permian (Rotliegendes) palaeowinds of the North Sea. *Sed. Geol.*, **34,** 245–265.

Glennie, K.W. (Ed.) (1998) *Petroleum Geology of the North Sea: Basic Concepts and Recent Advances*, 4th edn, Blackwell Science, Oxford, 636 pp.

Gradstein, F., Ogg, J.G. and **Smith, A.G.** (2004) *A Geologic Timescale*. Cambridge University Press, Cambridge.

Grant, S.F., Coe, A.L. and **Armstrong, H.A.** (1999) Sequence stratigraphy of the Coniacian succession of the Anglo-Paris Basin. *Geol. Mag.*, **136,** 17–38.

GRIP (Greenland Ice-core Project Members) (1993) Climate instability during the last interglacial period recorded in the GRIP ice core. *Nature*, **364,** 203–207.

Hiscott, R.N. (1981) Deep-sea fan deposits in the Macigno Formation (Middle-Upper Oligocene) of the Gordana Valley, northern Apennines, Italy – discussion. *J. Sed. Petrol.*, **51,** 1015–1033.

House, M.R. (1995) Orbital forcing timescales: an introduction. In: *Orbital Forcing Timescales and Cyclostratigraphy* (Eds M.R. House and A.S. Gale), *Geol. Soc. Spec. Publ.*, **67,** 1–18.

Howse, R. (1880) Note on the discovery in 1836-7 of a fossil fish (*Acrolepis kirkbyi*, n.s.) in the upper division of the Magnesian Limestone of Marsden. *Nat. Hist. Trans. Northumberland, Durham Newcastle-upon-Tyne*, **7,** 227–288.

Hughen, K.A., Overpeck, J.T., Peterson, L.C. and **Anderson, R.F.** (1996a) The nature of varved sedimentation in the Cariaco Basin, Venezuela and its palaeoclimatic significance. In: *Palaeoclimatology and Palaeoceanography from Laminated Sediments* (Ed. A.E.S. Kemp), *Geol. Soc. Spec. Publ.*, **116,** 171–183.

Hughen, K.A., Overpeck, J.T., Peterson, L.C. and **Trumbore, S.** (1996b) Rapid climate change in the Atlantic region during the last deglaciation. *Nature*, **380,** 51–54.

Hunt, D. and **Tucker, M.E.** (1992) Stranded parasequences and the forced regressive wedge systems tract: deposition during base-level fall. *Sed. Geol.*, **81,** 1–9.

Hunt, D. and **Tucker, M.E.** (1993) The sequence stratigraphy of carbonate shelves with an example from the Mid-Cretaceous of S.E. France. In: *Stratigraphy and Facies in a Sequence Stratigraphic Framework* (Eds. H.E. Posamentier, C.P. Sum-

merhayes, B.U. Haq and G.P. Allen), *Int. Assoc. Sedimentol. Spec. Publ.*, **18,** 307–341.

Huttel, P. (1989) Das Stassfurt-Karbonat (Ca2) in Süd-Oldenburg – fazies und diagenese eines sediments am Nordhang der Hunter-Schwelle. *Göttinger Arbeiten zur Geologie und Paläontologie*, **39,** vi + 94 pp. (+plates).

Johnsen, S.J., Clausen, H.B., Dansgaard, W., Fuhrer, K., Gundestrup, N., Hammer, C.U., Iversen, P., Jouzel, J., Stauffer, B. and **Steffensen, J.P.** (1992) Irregular glacial interstadials recorded in a new Greenland ice core. *Nature*, **359,** 311–313.

Kennet, J.P., Cannariato, K.G., Hendy, I.L. and **Behl, R.J.** (2000) Carbon isotopic evidence for methane instability during Quaternary interstadials. *Science*, **288,** 128–133.

Kirkby, J.W. (1863) Fossil fish in Magnesian Limestone at Fulwell Hill. *Trans. Tyneside Naturalists' Field Club* **5,** 248.

Kirkby, J.W. (1864) On some remains of fish and plants from the ''Upper Limestone'' of the Permian series of Durham. *Nat. Hist. Trans. Northumberland Durham* **1,** 64–83.

Kuhn, G. and **Meischner, D.** (1988) Quaternary and Pliocene turbidites in the Bahamas, Leg 101, sites 628, 632 and 635. In: *Proceedings of the Ocean Drilling Program, Scientific Results* (Eds J.A. Austin, W. Schlager *et al.*), *Ocean Drilling Program*, **101,** 203–212.

Kutzbach, J.E. (1994) Idealized Pangean climates: sensitivity to orbital change. In: *Pangea: Palaeoclimate, Tectonics, and Sedimentation during Accretion, Zenith, and Breakup of a Supercontinent* (Ed. G.D. Klein), *Geol. Soc. Am. Spec. Pap.*, **288,** 41–55.

Lehrmann, D.J. and **Goldhammer, R.K.** (1999) Secular variation in parasequence and facies stacking patterns of platform carbonates: a guide to application of stacking patterns analysis in strata of diverse facies and settings. In: *Advances in Carbonate Sequence Stratigraphy* (Eds P.M. Harris, A.H. Saller and J.A. Simo), *SEPM Spec. Publ.*, **63,** 187–225.

Leyrer, K., Strohmenger, C., Rockenbauch, K. and **Bechstaedt, T.** (1999) High-resolution forward stratigraphic modeling of Ca2-carbonate platforms and off-platform highs (Upper Permian, northern Germany). In: *Computerized Modeling of Sedimentary Systems* (Eds J. Harff, W. Lemke and K. Stattegger), pp. 307–339. Springer, Berlin.

Light, J.M. and **Wilson, J.B.** (1998) Cool-water carbonate deposition on the West Shetland shelf: a modern distally-steepened ramp. In: *Carbonate Ramps* (Eds V.P. Wright and T.P. Burchette), *Geol. Soc. Spec. Publ.*, **149,** 73–105.

Menning, M., Gast, R., Hagdorn, H., Käding, K.-C., Simon, T., Szurlies, M. and **Nitsch, E.** (2005) Zeitskala für Perm und Trias in der Stratigraphischen tabelle von Deutschland 2002, zylkostratigraphische kalibrierung der höheren Dyas und germanischen Trias und das alter der stufen Roadium bis Rhaetium 2005. *Newsl. Stratigr.*, **41,** 173–210.

Montañez, I.P., Tabor, N.J., Niemeier, D., DiMichele, W.A., Frank, T.D., Fielding, C.R., Isbell, J.L., Birgenheier, L.P. and **Rygel, M.C.** (2007) CO_2-forced climate and vegetation instability during Late Paleozoic deglaciation. *Science*, **315,** 87–91.

Mulder, T., Syvitski, J.P.M., Migeon, S., Faugères, J.-C. and **Savoye, B.** (2003) Marine hyperpycnal flows: initiation, behaviour and related deposits. A review. *Mar. Petrol. Geol.*, **20,** 861–882.

Murray, C.J., Lowe, D.R., Graham, S.A., Martinez, P.A., Zeng, J., Carroll, A.R., Cox, R., Hendrix, M., Heubeck, M., Miller, D., Moxon, I.W., Sobel, E., Wendebourg, J. and **Williams, T.** (1996) Statistical analysis of bed-thickness patterns in a turbidite section from the Great Valley sequence, Cache Creek, northern California. *J. Sed. Petrol.*, **66,** 900–908.

Nott, J. and **Hayne, M.** (2001) High frequency of 'super-cyclones' along the Great Barrier Reef over the past 5,000 years. *Nature*, **413,** 508–512.

Peryt, T.M. (1986) The Zechstein (Upper Permian) Main Dolomite deposits of the Leba Elevation, northern Poland: facies and depositional history. *Facies*, **14,** 151–200.

Pettigrew, T. (1980) Geology. In: *The Magnesian Limestone of Durham County* (Ed. T.C. Dunn), pp. 6–26. Durham County Conservation Trust, Durham.

Pickering, K.T., Hiscott, R.N. and **Hein, F.J.** (1989) *Deep Marine Environments: Clastic Sedimentation and Tectonics*. Unwin Hyman, London, x + 416 pp.

Rees, P.McA., Gibbs, M.T., Ziegler, A.M., Kutzbach, J.E. and **Behling, P.J.** (1999) Permian climates: evaluating model predictions using global paleobotanical data. *Geology*, **27,** 891–894.

Rees, P.McA., Ziegler, A.M., Gibbs, M.T., Kutzbach, J.E., Behling, P.J. and **Rowley, D.B.** (2002) Permian phytogeographic patterns and climate data/model comparisons. *J. Geol.*, **110,** 1–31.

Reijmer, J.J.G., Sprenger, A., Ten Kate, W.G.H.Z., Schlager, W. and **Krystyn, L.** (1994) Periodicities in the composition of Late Triassic calciturbidites (eastern Alps, Austria). In: *Orbital Forcing and Cyclic Sequences* (Eds P.L. De Boer and D.G. Smith), *Int. Assoc. Sedimentol. Spec. Publ.*, **19,** 323–343.

Reuning, L., Reijmer, J.J.G., Betzler, C., Timmermann, A. and **Steph, S.** (2006) Sub-Milankovitch cycles in periplatform carbonates from the early Pliocene, Great Bahama Bank. *Paleoceanography*, **21,** 1–11.

Rhys, G.H. (1974) A proposed standard lithostratigraphic nomenclature for the southern North Sea and an outline structural nomenclature for the whole of the (UK) North Sea. Institute of Geological Sciences Report, 74/8. HMSO, London, 14 pp.

Richter-Bernburg, G. (1955) Stratigraphische gliederung des Deutschen Zechsteins. *Zusammen Deutschlands Geologisches Gesellschaft*, **105,** 593–645.

Rohling, E.J., Grant, K., Hemleben, Ch., Siddall, M., Hoogakker, B.A.A., Bolshaw, M. and **Kucera, M.** (2007) High rates of sea-level rise during the last interglacial period. *Nature Geosci.*, **1,** 38–42.

Roth, S. and **Reijmer, J.J.G.** (2005) Holocene millennial to centennial carbonate cyclicity recorded in slope sediments of the Great Bahama Bank and its climatic implications. *Sedimentology*, **52,** 161–181.

Schlager, W. (1992) *Sedimentology and sequence stratigraphy of reefs and carbonate platforms*. American Association of Petroleum Geologists Continuing Education, Short Course Notes no. 34, AAPG, Tulsa, 71 pp.

Schlager, W., Reijmer, J.J.G. and **Droxler, A.** (1994) Highstand shedding of carbonate platforms. *J. Sed. Res.*, **64,** 270–281.

Scholle, P.A., Arthur, M.A. and **Ekdale, A.A.** (1983) Pelagic environment. In: *Carbonate Depositional Environments* (Eds P.A. Scholle, D.G. Bebout and C.H. Moore), *AAPG Mem.*, **33,** 619–692.

Schulz, H., von Rad, U. and **Erienkeuser, H.** (1998) Correlation between Arabian Sea and Greenland climate oscillations of the past 110,000 years. *Nature*, **393,** 54–57.

Shanmugam, G. (2008) The constructive functions of tropical cyclones and tsunamis on deep-water sand deposition during sea-level highstand: implications for petroleum exploration. *AAPG Bull.*, **92,** 443–471.

Smith, D.B. (1989) The late Permian palaeogeography of north-east England. *Proc. Yorkshire Geol. Soc.*, **47,** 285–312.

Smith, D.B. (1994) Geology of the Country around Sunderland. Memoir for 1:50,000 Geological Sheet 21 (England and Wales). British Geological Survey, HMSO, London, xi + 161 pp.

Smith, D.B. and **Francis, E.A.** (1967) *Geology of the Country between Durham and West Hartlepool. Memoir of the Geological Survey of Great Britain, Sheet 27 (England and Wales).* HMSO, ??????, xiii + 354 pp.

Smith, D.B. and **Taylor, J.C.M.** (1992) Permian. In: *Atlas of Palaeogeography and Lithofacies* (Ed. J.C.W. Cope), *Geol. Soc. Mem.*, **13,** 87–96.

Southgate, P.N., Kennard, J.M., Jackson, M.J., O'Brien, P.E. and **Sexton, M.J.** (1993) Reciprocal lowstrand clastic and highstrand carbonate sedimentation, subsurface Devonian reef complex, Canning Basin, Western Australia. In: *Carbonate Sequence Stratigraphy: Recent Developments and Applications* (Eds R.G. Loucks and J.F. Sarg). *AAPG Mem.*, **57,** 157–180.

Steinhoff, I. and **Strohmenger, C.** (1996) Zechstein 2 carbonate platform subfacies and grain-type distribution (Upper Permian, northwest Germany). *Facies*, **35,** 105–132.

Stow, D.A.V., Reading, H.G. and **Collinson, J.D.** (1996) Deep seas. In: *Sedimentary Environments: Processes, Facies and Stratigraphy* (Ed. H.G. Reading), 3rd edn. pp. 395–453. Blackwell Science, Oxford.

Strohmenger, C., Voigt, E. and **Zimdars, J.** (1996a) Sequence stratigraphy and cyclic development of Basal Zechstein carbonate-evaporite deposits with emphasis on Zechstein 2 off-platform carbonates (Upper Permian, Northeast Germany). *Sed. Geol.*, **102,** 33–54.

Strohmenger, C., Antonini, M., Jäger, G., Rockenbach, K. and **Strauss, C.** (1996b) Zechstein 2 carbonate reservoir facies distribution in relation to Zechstein sequence stratigraphy (Upper Permian, northwest Germany): an integrated approach. *Bulletin Centres Recherches Exploration – Production Elf Aquitaine*, **20,** 1–35.

Sylvester, Z. (2007) Turbidite bed thickness distributions: methods and pitfalls of analysis and modelling. *Sedimentology*, **54,** 847–870.

Taylor, J.C.M. (1998) Upper Permian – Zechstein. In: *Petroleum Geology of the North Sea: Basic Concepts and Recent Advances* (Ed K.W. Glennie), 4th edn. pp. 174–211. Blackwell Science, Oxford.

Taylor, J.C.M. and **Colter, V.S.** (1975) Zechstein of the English sector of the southern North Sea. In: *Petroleum of the Continental Shelf of North-West Europe* (Ed A.W. Woodland), pp. 249–263. Institute of Petroleum, London.

Thompson, W.G. and **Goldstein, S.L.** (2005) Open-system coral ages reveal persistent suborbital sea-level cycles. *Science*, **308,** 401–404.

Tucker, M.E. (1991) Sequence stratigraphy of carbonate-evaporite basins: models and applications to the Upper Permian (Zechstein) of northeast England and adjoining North Sea. *J. Geol. Soc. London* **148,** 1019–1036. (also discussion: *J. Geol. Soc. London*, 149, 1050–1054).

Tucker, M.E. (2003a) *Sedimentary Rocks in the Field*, 3rd edn. John Wiley, Chichester, 234 pp.

Tucker, M.E. (2003b) Mixed clastic-carbonate cycles and sequences: Quaternary of Egypt and Carboniferous of England. *Geol. Croatica*, **56,** 19–37.

Tucker, M.E., Gallagher, J. and **Leng, M.** (2009) Are beds in shelf carbonates millennial-scale cycles? An example from the mid-Carboniferous of NE England. *Sed. Geol.*, **214,** 19–34.

Van der Baan, D. (1990) Zechstein reservoirs in the Netherlands. In: *Classic Petroleum Provinces* (Ed. J. Brooks), *Geol. Soc. Spec. Publ.*, **50,** 379–398.

Ward, P.L. (2009) Sulfur dioxide initiates global climate change in four ways. *Thin Solid Films*, **517,** 3188–3203.

Wilson, P.A. and **Roberts, H.H.** (1992) Carbonate-periplatform sedimentation by density flows: a mechanism for rapid off-bank and vertical transport of shallow-water fines. *Geology*, **20,** 713–716.

Wilson, P.A. and **Roberts, H.H.** (1995) Density cascading: off-shelf sediment transport, evidence and implications, Bahama Banks. *J. Sed. Res.*, **65,** 45–56.

Yancheva, G., Nowacyzk, N.R., Mingram, J., Dulksi, P., Schettler, G., Negendank, J.F.W., Liu, J., Sigman, D.M., Peterson, L. and **Haug, G.H.** (2007) Influence of the intertropical convergence zone on the East Asian monsoon. *Nature*, **445,** 74–77.

Ziegler, A.M. (1990a) Phytogeographic patterns and continental configurations during the Permian period. In: *Palaeozoic Palaeogeography and Biogeography* (Eds W.S. McKerrow and C.R. Scotese) *Geol. Soc. Mem.*, **12,** 363–379.

Ziegler, P.A. (1990b) *Geological Atlas of Western and Central Europe*, 2nd edn. Shell International, The Hague. pp. 239 + 56 enclosures (in 2 volumes).

Ziegler, A.M., Hulver, M.L. and **Rowley, D.B.** (1997) Permian world topography and climate. In: *Late Glacial and Postglacial Environmental Changes: Quaternary, Carboniferous-Permian and Proterozoic* (Ed. I.P. Martini), pp. 111–146. Oxford University Press, Oxford.

Zühlke, R. (2004) Integrated Cyclostratigraphy of a Model Mesozoic Carbonate Platform - the Latemar (Middle Triassic, Italy). In: *Cyclostratigraphy. An Essay of Approaches and Case Histories* (Eds B. D'Argenio, A. Fisher, I. Premoli Silva and H. Weissert). *Soc. Sed. Geol. Spec. Publ.*, **81,** 183–212.

Manuscript received 28 April 2008; revision accepted 19 February 2009

APPENDIX

Nomenclature of Zechstein Cycle 2 carbonates in North-east England: Reasons for change:

1. In many instances, the facies of the two formations into which the Z2C was previously divided, are hard to discriminate. Shallow-water facies, typified by oolite, were assigned to the Roker Dolomite. Slope-apron facies, characterized by those described in this study, and middle-ramp facies such as ribbon rocks, comprised the Concretionary Limestone. Many facies in the Roker Formation are, however, difficult to interpret and have characteristics typical of either formation. Concretionary fabrics from dedolomitization, for which the Concretionary Limestone was named, are not always present and do occur in the Zechstein Cycle 3 Seaham Formation, as well.

2. The Z2C does not show the simple shallowing-upward succession and facies partitioning understood to be present when the two formations were established. Facies analysis shows a more complicated pattern in which, as mentioned in this paper, at least three smaller-scale packages are present.

3. Thus it is recommended that the terms Roker Dolomite and Concretionary Limestone be abandoned and replaced by the term Roker Formation.

